

**A Center for Advanced Materials and Nanotechnology in AMRI  
at the University of New Orleans**

**Louisiana Board of Regents Contract  
LEQSF(2007-12)-ENH-PKSFI-PRS-04**

**Annual Progress Report - 2010**

**June 30, 2010**

**SUMMARY**

The purpose of this report is to provide an annual progress report for the LA Board of Regents funded project entitled: “A Center for Advanced Materials and Nanotechnology in AMRI at the University of New Orleans” through LA Board of Regents Contract LEQSF(2007-12)-ENH-PKSFI-PRS-04 during the third year of the project from July 1, 2009, through June 30, 2010. Included are progress reports from the three Focus Research Groups (FRGs) and the Broader Impacts group which comprise the organization of the overall project, plus a progress report on the Clean Room Project for which received ESIP funds for development of a Nanodevice Processing Laboratory to support ongoing research projects in nanotechnology at UNO.

The third year of this project was very productive and has been successfully completed. A research consortium organization for this project continues in place and includes as participants the University of New Orleans and the following five partner institutions: Louisiana State University, Tulane University, Louisiana Tech University, Children’s Hospital, and Communities in Schools of New Orleans, Inc. The subcontracts from the University of New Orleans to the five collaborating partner institutions continue in place and the work at these institutions is progressing well. The overall effort of the project is organized into three FRGs based on technical areas and one Broader Impacts group, which provides community outreach support for the project. These groups are: FRG-1: Nanomaterials for Biological Sensing and Imaging; FRG-2: Nanoscale Mechanical Devices; FRG-3: Nanomaterials for Energy Conversion and Storage; and the Broader Impacts (Educational and Commercial Outreach) group. All research activities within each group are progressing well.

The overall project management for this program is melded into AMRI’s existing management and review structure as follows. Each year, all P-KSFI teams hold a comprehensive annual review in conjunction with the Annual AMRI Mardi Gras Review and Symposium. Invited to participate in this review are the members of the AMRI Technical Advisory Board (TAB) and review teams from the funding agencies. In addition to this meeting, there are one-day AMRI review meetings for the other three quarters in the year where the teams and investigators present their research and discuss strategies.

Once a month one of the Focused Research Groups (FRGs) in this program holds a meeting and all researchers in the consortium are encouraged to attend these meetings so that all are aware of what each group is doing. This promotes cross-fertilization of ideas and helps to further expand

the pool of expertise available within these groups. The basic management tasks at this level (FRG) is to facilitate communication, minimize the administrative burden on the faculty and to mentor the junior faculty in writing large, multi-PI grant proposals and effectively handling intellectual property (IP) issues. This is accomplished using video conferencing facilities and coordinating the quarterly meetings with the lead PI. The AMRI multi-investigator meetings are currently held on each Thursday afternoon with a different multi-investigator group presenting their work each week. The research groups of all co-investigators also hold their own group meetings, usually once a week.

The PKSFI researchers participate in a monthly meeting where research progress, issues and potential collaborations are discussed. The responsibility for the meeting rotates between the individual Focused Research Groups (FRGs) and the Broader Impacts group. A researcher (co-PI, post-doc or student) typically gives a 20-40 min presentation followed by discussion. All AMRI researchers are encouraged to attend the meetings including those not part of the PKSFI program. Table 1 below lists the meetings held in year 3 (2009-2010).

**Table 1. PKSFI Monthly UNO group Meetings for 2009-2010.**

<b>DATE</b>	<b>GROUP</b>	<b>SPEAKER</b>	<b>TOPIC</b>
June 25, 2009	FRG 3	K. Stokes	Progress in Nanophase Bismuth Telluride
August 27, 2009	FRG 2	L. Spinu/V.J. John	Novel Fe-Carbon Composites with Applications to Environmental Remediation, Bioseparation and Magnetic Materials
September 24, 2009	Broader Impacts	M. Tarr	Outreach Programs in Development
October 22, 2009	FRG 3	L. Malkinski	Bulk Multiferroic Composites and New approaches to Voltage-Controlled Magnetism
January 28, 2010	FRG 1	S.Rai	Synthesis and Characterization of PC/PMMA Blend Nanocomposite
February 25, 2010	FRG 2	J. Wiley	Recent Results in Polymer Nanowires
March 25, 2010	FRG 3	N. Henderson	Chemical Synthesis of Ag and Ag <sub>2</sub> Te Nanoparticles for Thermoelectric Nanocomposites
April 22, 2010	FRG 1	H.Qu	Synthesis of Fe <sub>3</sub> O <sub>4</sub> nanoparticles with different surface functionality
May 27, 2010	Broader Impacts	M. Tarr/K. Stokes	A First-Hand Look at the Gulf of Mexico Oil Spill
June 24, 2010	FRG 2	J. Wiley	Curls and Swirls in Polymer Wires

## Report for LEQSF(2010-06)-ENH-PKSFI-PRS-04

Weilie Zhou

(PKSFI FRG 1, 2009-2010)

### FRG-1: Nanomaterials for Biological Sensing and Imaging

#### UNO-AMRI

**1. Personnel:** personnel involves with this project

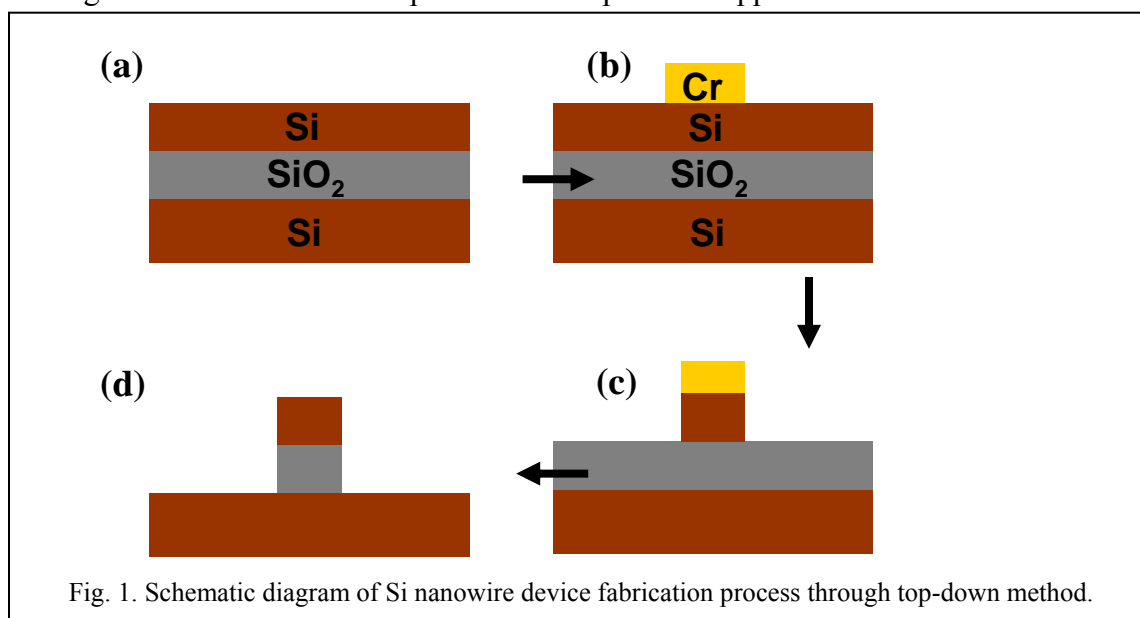
- **Weilie Zhou-** co-Leader of FRG 1. He is mainly responsible for overall management for biosensor part and coordination of AMRI tasks with other partners
- **Kun Yao-**Postdoctoral Research Associate. He is in charge of nanowire FET design, fabrication, and detection of antigen fabricated from Children Hospital of LSUHSC.
- **Hui Ma-**Ph.D student. She is fabricating magnetic nanocarriers for drug delivery and meanwhile she is in charge of modifying the nanowire surface for bio-detection.

#### 2. Activities and Findings:

##### I. Nanowire FET fabrication for biosensor application

We have shown the  $\text{In}_2\text{O}_3$  nanowire field-effect transistors (FET) by bottom-up method in the last report. We also worked on Si nanowire FET by top-down method this year, because it is more compatible with modern semiconductor manufacturing techniques and potential for large scale integration. Furthermore, we can precisely design the position of the nanowire without imperfect alignment issue which most happens in bottom-up method.

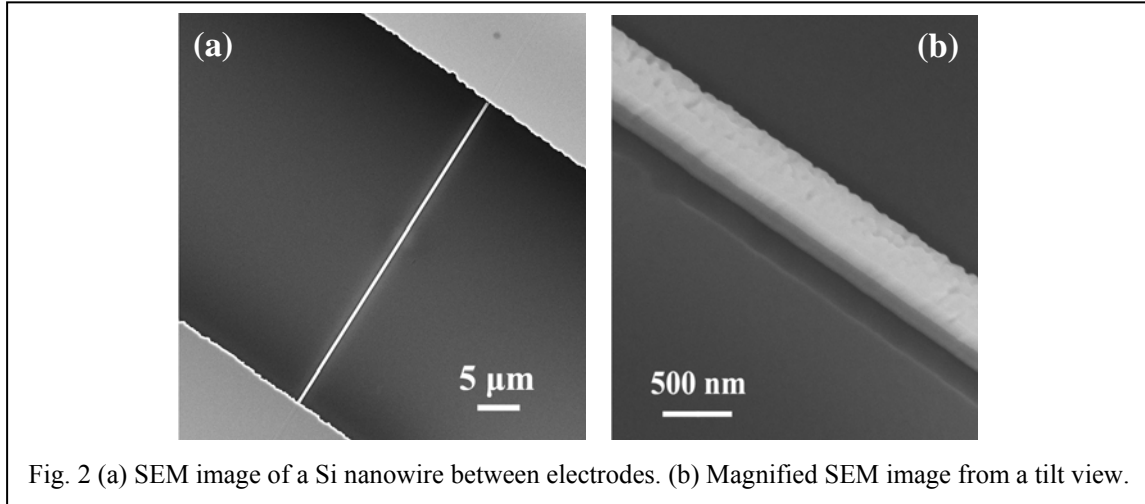
Figure 1 illustrates the process of top-down approach to fabricate Si nanowire,



summarized as follows: a) Starting with silicon-on-insulator (SOI) wafer that consists of a 380nm buried oxide layer and a 100~280 nm silicon layer on insulator; b) Cr mask fabrication

by e-beam patterning, Cr metal deposition and liftoff process; c) Silicon etching by a reactive ion etching (RIE) system; d) Cr mask remove by Cr etching solution.

Figure 2a shows SEM image of a Si nanowire between two predefined electrodes and Figure 2b shows the magnified SEM image from a tilt view. The roughness of the Si surface comes from the etching processes. However, we found obvious current leakage from test between Si nanowire and the bottom Si layer, which might result from the residues during RIE etching process and definitely degraded the performance of Si nanowire FET.



Jointly with researchers at CAMD initial efforts optimizing the etching procedures have been started. If the etching time is not enough, the Si layer would etch incompletely. In contrast the insulator layer ( $\text{SiO}_2$ ) may remove partially, worsening the dielectric properties of nanowire devices. Initial etching conditions were using an ICP power of 600 W, an Rf power of 15W, and a pressure of 20mtorr with  $\text{CF}_4$  as etch gas. The results are shown in Figs. 3 clearly stating that more process optimization is required to achieve smooth sidewalls of the channel/wire structures.

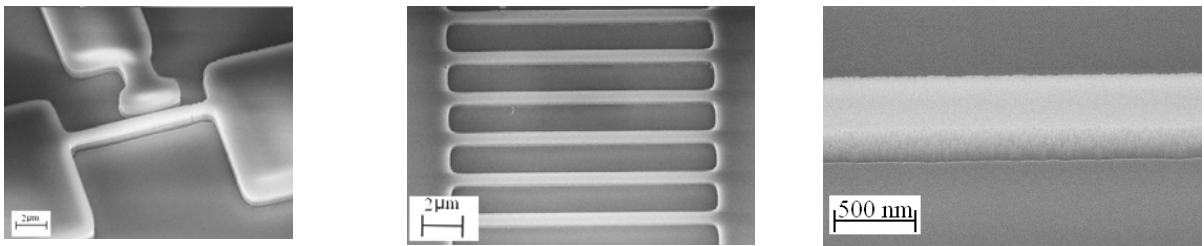


Fig. 3: Examples of etched nanowires and channels, the Cr layer was nearly etched away allowing the gas to attack the covered silicon layer and also partly the  $\text{SiO}_2$  layer.

Further improvement in the etching process is illustrated in Figures 4 showing different surface conditions after DRIE etching between the photoresist (PR) etch mask and an optimized Cr mask on Au/Cr/SOI wafer. In Fig 4, left even though a very thick PR ( $\sim 1.5\mu\text{m}$ ) etch mask was used the surface showed surface charging on SEM picture indicating oxidation and potentially influencing the Si NW characteristics. Fig. 4, right shows a much higher etch selectivity for the Cr mask compared to the PR mask. The selectivity was  $> 80:1$  of Si: Cr.

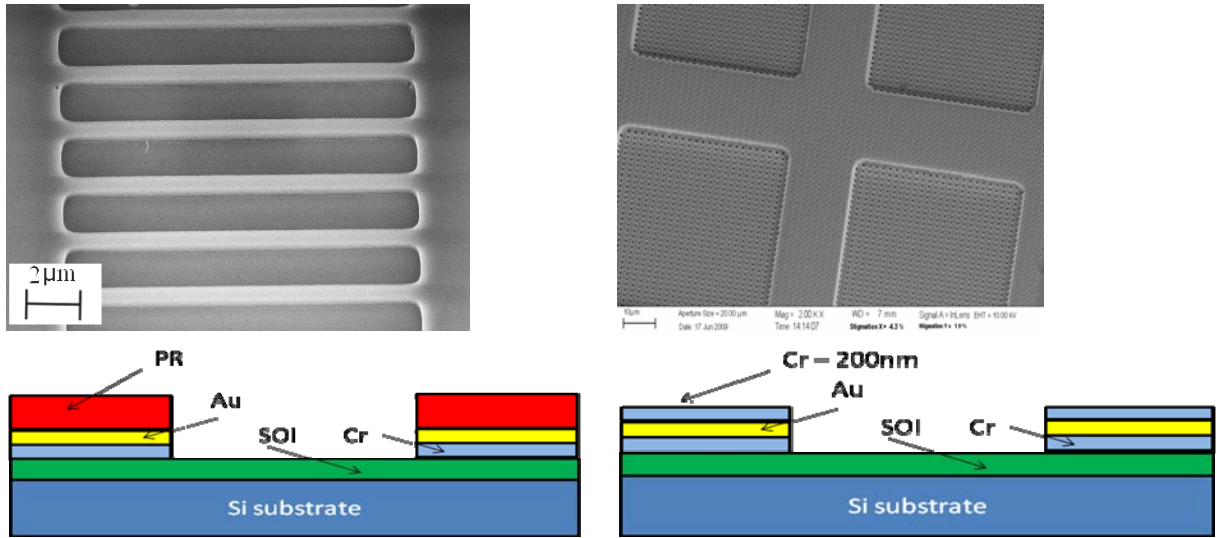


Figure 4: Surface condition difference after DRIE between the photoresist mask (left) and the Cr mask (right) on Au/Cr/SOI wafer. The schematic illustrates the respective etch mask configuration.

Another issue associated with the etching process is the non-uniformity of DRIE etching due to different feature-scales on a typical etch sample ranging from millimeters to nanometers (Fig.5).

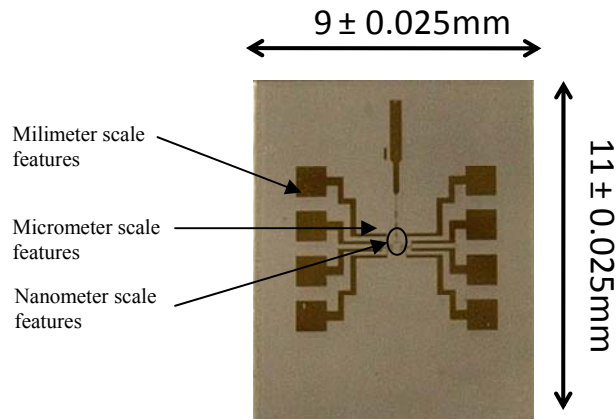


Fig. 5: Typical electrodes patterns

As a preliminary result optimum process results has been achieved using alternative process recipes of two different rf powers of 15W and 50W, respectively. The other etching conditions are ICP power of 400 W, substrate temperature of 35 °C and pressure of 20 mtorr with etch-gas  $\text{CF}_4$  of 30 sccm. Pictures in Fig. 6 show the etching uniformity controlling by alternating rf power 15W to 50W for 1 minute respectively. Total etching time was 6 minutes.

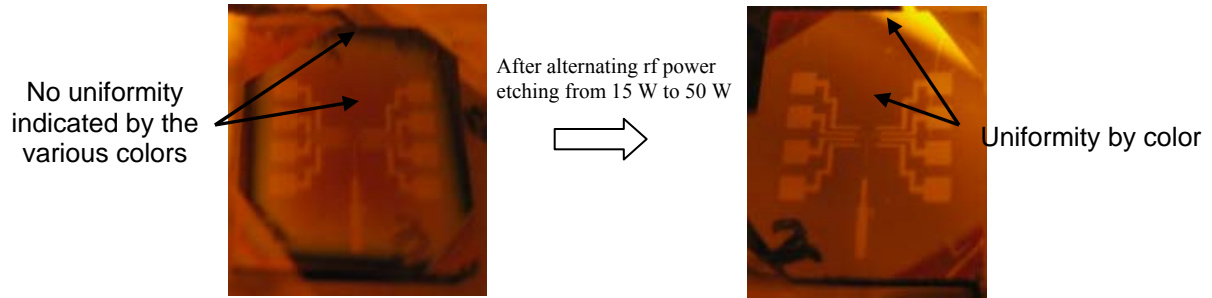


Fig. 6 DRIE etching SOI samples

In future work, we will further address the process related issues and optimize the etching procedure.

## II. Surface modification engineering

The simple concept and mechanism of nanowire FET based biosensor is shown in Figure 7, where the current flowing through the nanowire channel (orange part), as the sensing signal, can be modulated by the electric field derived from the attached molecules (pink part). For bonding the target bio-molecules to the nanowire, medium molecules (blue part) are usually needed, consisting of one kind of molecule or several kinds of molecules connecting one by one. Such binding process should also be reversible by buffer solutions [1].

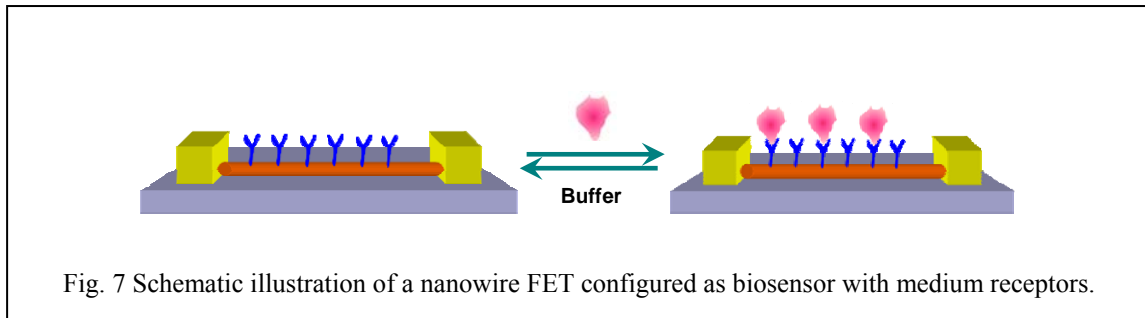


Fig. 7 Schematic illustration of a nanowire FET configured as biosensor with medium receptors.

Figure 8 shows an example structure of the medium molecules (blue part in Fig 3) with backbone, variable portion for binding to bio-molecules and engineered tag for binding to nanowire [2]. So far we consider several candidates for the engineered tag such as lysine, histidine, cysteine.

The surface modification engineering work is based on  $\text{In}_2\text{O}_3$  nanowire FET which we have studied for a long time. In our design, 6-Phosphonohexanoic acid will binding on  $\text{In}_2\text{O}_3$  nanowire surface by stirring in aqueous solution, followed by attaching medium molecules (mostly lysine tagged antibody). To ensure the series of binding, we need to figure out some methods to monitor them step by step. For the first step to verify the binding of 6-Phosphonohexanoic acid, 4-aminobenzoic acid (PABA) were linked to the tip of 6-Phosphonohexanoic acid under catalysis (EDC) because PABA can be detected by UV absorbance, which is shown in Figure 9a. Figure 9b demonstrates the UV absorbance of contrastive samples, where both the position and intensity of the peak from PABA attached nanowire matches PABA solution very well and proves the successful binding.

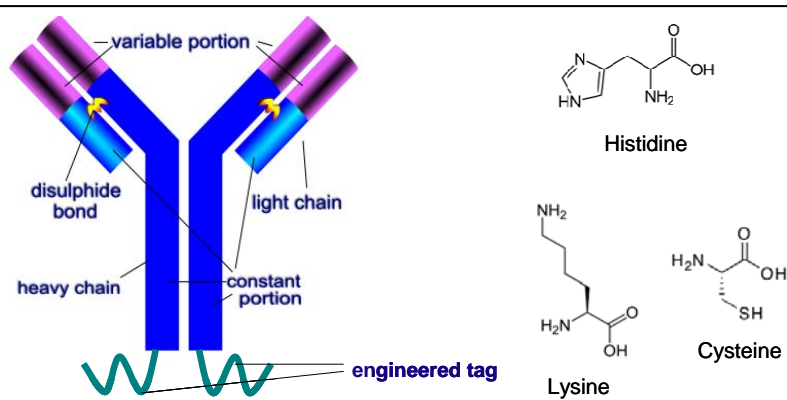


Fig. 8. Example structure of the medium molecules.

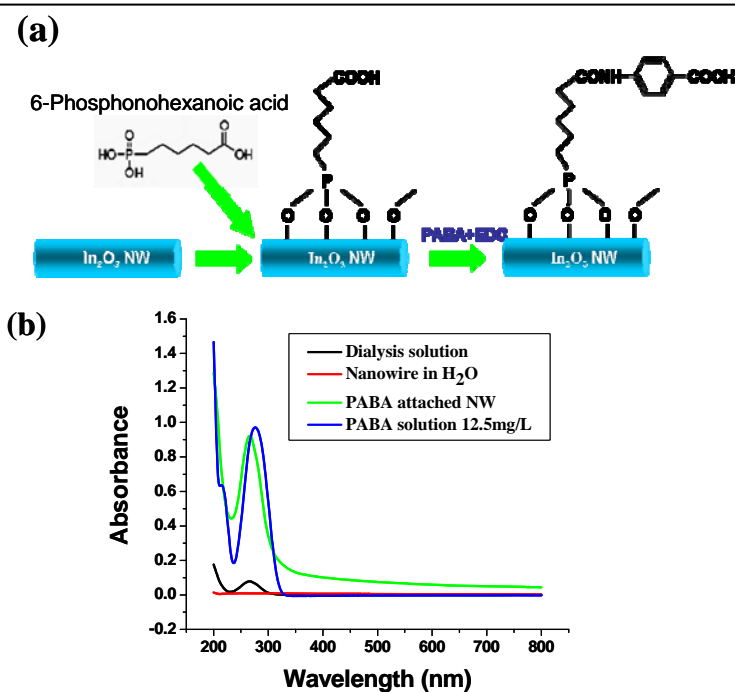


Fig. 9 (a) Schematic illustration of  $\text{In}_2\text{O}_3$  nanowire attached with 6-Phosphonohexanoic acid and then PABA. (b) UV absorbance of contrastive samples showing the successful binding.

## Reference

- [1] Patolsky, F.; Zheng, G.; Lieber, C. M. *Nanomedicine* **2006**, *1*, 51
- [2][http://upload.wikimedia.org/wikipedia/commons/thumb/f/f6/Antibody\\_svg.svg/339px-Antibody\\_svg.svg.png](http://upload.wikimedia.org/wikipedia/commons/thumb/f/f6/Antibody_svg.svg/339px-Antibody_svg.svg.png)

## Publication

1. Kun Yao, Daniela Caruntu, Zhongming Zeng, Jiajun Chen, Charles J. O'Connor, Weilie Zhou, **J. Phys. Chem. C** 113, 14812, 2009, "Ppb level H<sub>2</sub>S Detection at Room Temperature Based on Self-Assembled In<sub>2</sub>O<sub>3</sub> Nanoparticles".
2. Kun Yao, Daniela Caruntu, Baobao Cao, Charles J. O'Connor, Weilie Zhou, accepted by **IEEE Trans. Nanotechnol**, 2010, "Investigation of Gas Sensing Performance of SnO<sub>2</sub> Nanoparticles with Different Morphologies".
3. Daniela Caruntu, Kun Yao, Zengxing Zhang, Tabitha Austin, Weilie Zhou, Charles J. O'Connor, **J. Phys. Chem. C** 114, 4875, 2010, "One-Step Synthesis of Nearly Monodisperse, Variable-Shaped In<sub>2</sub>O<sub>3</sub> Nanocrystals in Long Chain Alcohol Solutions".

## Presentation

1. Kun Yao, Daniela Caruntu, Charles J. O'Connor, Weilie Zhou, "Ppb Level Gas Detection at Room Temperature Based on Self-Assembled Indium Oxide Nanoparticles", **2009 Nanoelectronic Devices for Defense & Security (NANO-DDS) Conference**, Ft. Lauderdale, Florida, USA, Sept. 28~ Oct. 2. (Oral Presentation)
2. Hui Ma, Zhongming Zeng, Yoon Young Jin, Jost S. Goettert, Seth Pincus, and Weilie Zhou, "Semiconductor Nanowire Transistor for Biosensor Detection", **2009 Nanoelectronic Devices for Defense & Security (NANO-DDS) Conference**, Ft. Lauderdale, Florida, USA, Sept. 28~ Oct. 2. (Poster Presentation)
3. Kun Yao, Zhijie Li, and Weilie Zhou, "Synthesis and sensing investigation of new coordination compounds nanowires", **The 3<sup>rd</sup> International Conference on One-dimensional Nanomaterials**, Atlanta, Georgia, USA, December 7-9, 2009. (Poster Presentation)
4. Hui Ma, Zhongming Zeng, Yoon Young Jin, Jost S. Goettert, Seth Pincus, and Weilie Zhou, "Surface modification of silicon nanowire array for selective biosensor detection", **The 3<sup>rd</sup> International Conference on One-dimensional Nanomaterials**, Atlanta, Georgia, USA, December 7-9, 2009. (Poster Presentation)
5. Kun Yao, Daniela Caruntu, Zhongming Zeng, Jiajun Chen, Baobao Cao, Charles J. O'Connor, and Weilie Zhou, "Parts per Billion-Level Gas Detection at Room Temperature Based on Self-Assembled Nanoparticles", **Annual AMRI Mardi Gras Review and Symposium**, New Orleans, Louisiana, USA, February 11-12, 2010. (Poster Presentation)
6. Hui Ma, Zhongming Zeng, Yoon Young Jin, Jost S. Goettert, Seth Pincus, and Weilie Zhou, "In<sub>2</sub>O<sub>3</sub> Nanowire Based Field-Effect Transistor for Ricin Detection", **Annual AMRI Mardi Gras Review and Symposium**, New Orleans, Louisiana, USA, February 11-12, 2010. (Poster Presentation)



## **LSU-CAMD**

### **1. Personnel:**

#### **Senior staff** (entire time)

- Jost Goettert
- Yoonyoung Jin

#### **Student support** (entire time)

- Kyung-Nam Kang (thin-film deposition, Si etching, optical lithography)

#### **Part time on this project**

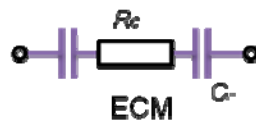
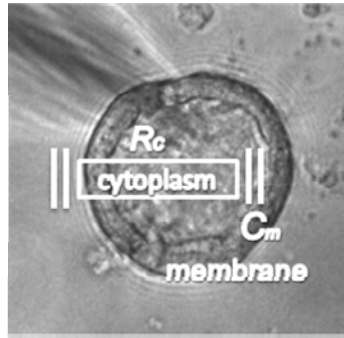
- Proyag Datta (until 10/2010)
- Niklas Frische (until 9/2010)
- Sital Tiwari (part time, molding support since 10/2010)
- Jeonghwan Kim (part time, microfluidic, since 10/2010)

#### **Summary**

The efforts in the past year were focusing on three areas. Two areas were related to further develop the microfluidic stack and expand its potential while the other effort was a close collaboration with AMRI researchers to develop top-down nanowire sensor modules.

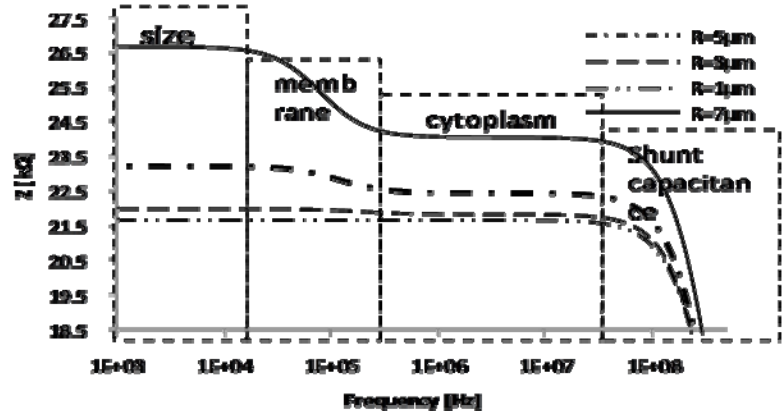
#### **Fluidic stack solution for cell sorting application**

This effort was aimed to bring together all previous efforts and build a complete module that controls a fluidic flow and detects cells passing across the electrode area. The idea for cell sorting is based on the fact that a cell can be represented by resistivity and capacity and that electrodes embedded in a fluidic channel experience a change of impedance when a cell is passing by. This impedance change generates an electrical signal characteristic for the particular cell (for example size) and can be used to trigger a fluidic flow manipulation allowing to selectively extracting the cell. Fig. 1 summarizes the fundamental idea and illustrates that sensing with high frequencies in the kHz to MHz range allows using different cell properties for selection while Fig. 2 presents the basic idea of how the cell sorting in a continuous flow is realized.



$$Z = R_c - j \frac{2}{2\pi C_m} \times \frac{1}{f}$$

Frequency dependent



Cell counting

characterization by size and dielectric properties

distinguish between healthy, dead or damaged cells

Fig. 1: Electrical representation of a cell and calculated impedance change for different frequencies representing different cell characteristics suitable for cell selection.

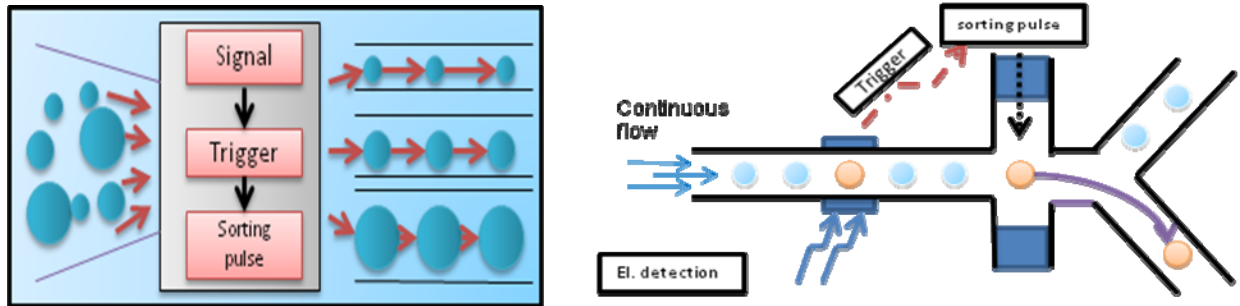


Fig. 2: Representation of the basic sorting concept – a continuous of cells with different size/properties is passing the electrode setup and generates a trigger pulse that will be used to sort out the cells with pre-defined characteristics.

The experimental setup used in this experiment is illustrated in Fig. 3. The fluidic stack was assembled, connected to the electrical and fluid control units, and placed under an optical microscope for in-situ inspection allowing correlating the electrical signal with a visual impression. While the stack is truly a MEMS size device all peripheral equipment like syringe pumps, electrical signal generator, and data acquisition unit have not been miniaturized at this point.

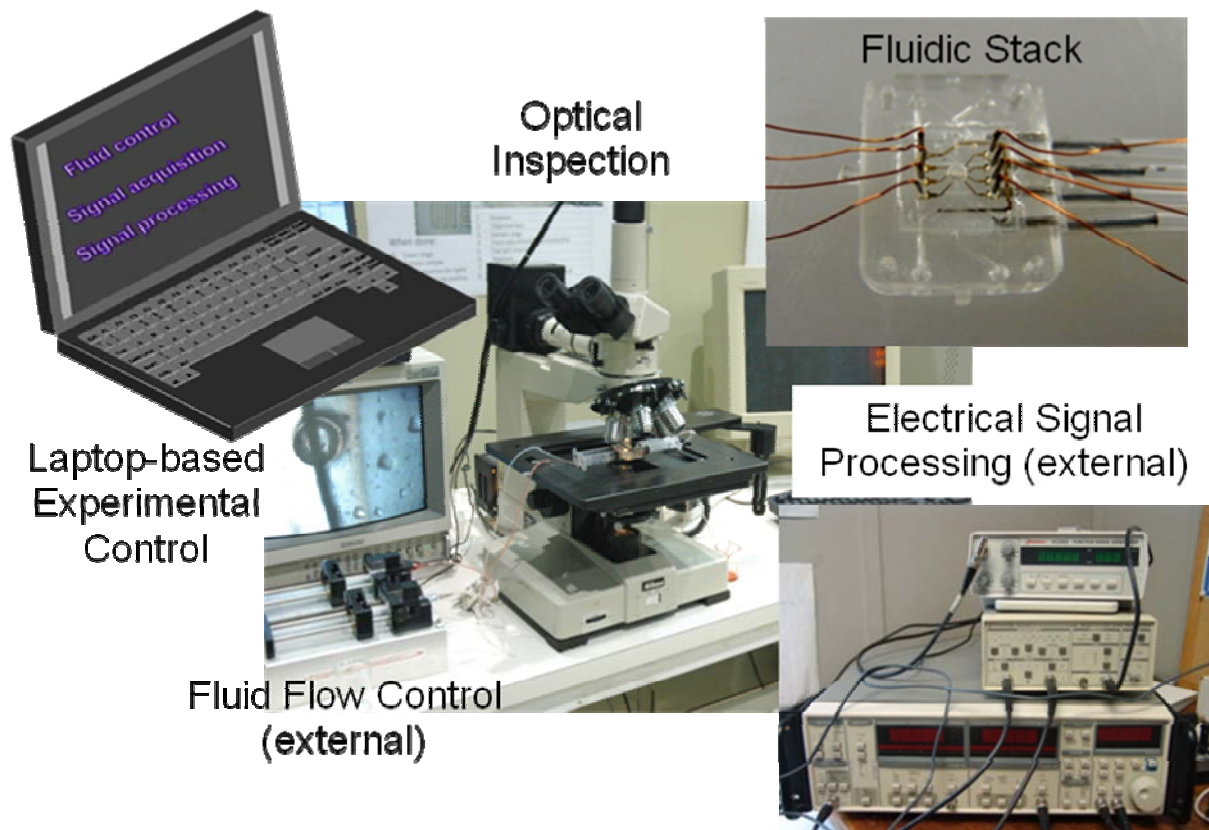


Fig. 3: Experimental setup for initial cell sorting experiments.

The fluidic stack consists of different functional modules described in last year's reports. One important fluidic module is a hydrodynamic focusing module which allows focusing and manipulating the sample carrying liquid (see Fig. 4). This prevents agglomeration of cells by sticking to the channel sidewalls and ultimately clogging it (see Fig. 5).

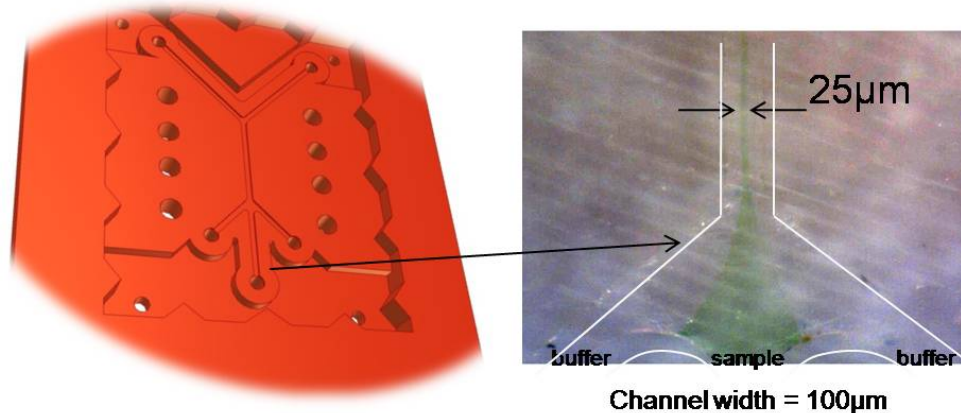


Fig. 4: Design of the hydrodynamic focusing module (left) and successful focusing the sample stream (made visible by green food color) to about 25μm width while flowing through a ~100μm wide channel (right).

### Cell agglomeration in microchannels with time results in blocking

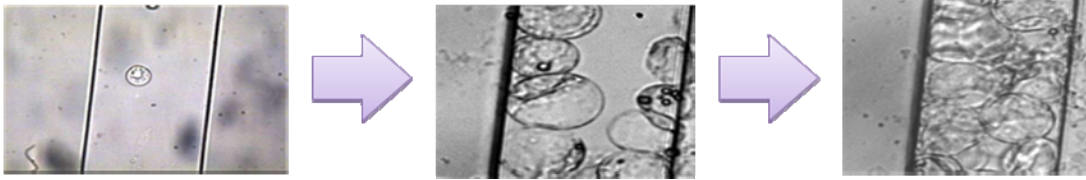


Fig. 5: Example of channel clogging over time when running typical cell samples through the  $\sim 100\mu\text{m}$  wide channel.

A test run using polystyrene microspheres of different sizes was conducted illustrating the successful generation of characteristic electrical signals for spheres of different sizes (see Fig. 6).

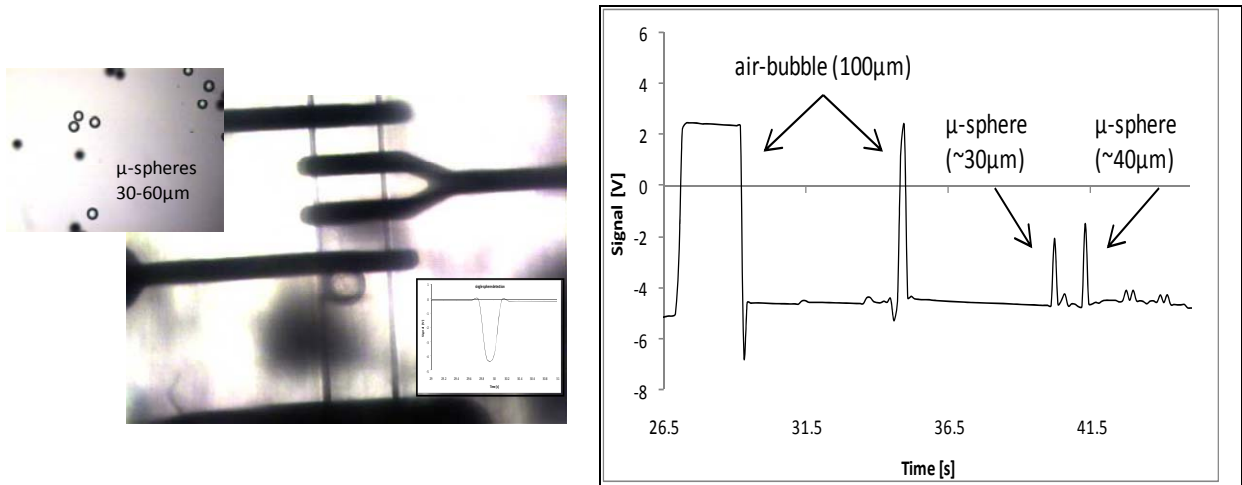


Fig. 6: The picture to the left shows the electrode arrangement inside a fluidic channel with a sphere of  $\sim 60\mu\text{m}$  width passing by and measured signals generated by spheres of different size (right). A problem still to be addressed are air bubbles that cover the entire channel width and cause a maximum signal of about 7V.

Achieving an electrical signal using laboratory-size electronic and fluidic control equipment demonstrates that in principle all key functions of the stack are working and allow detection of electrical signals generated within the microfluidic stack. Research described in more detail in the thesis from Niklas Frische (N. Frische, "Microfluidic impedance spectroscopy module for label-free particle sensing and counting, Bachelor Thesis Fachhochschule Gelsenkirchen, June 2009) shows, however that much more efforts need to be invested in the development of miniaturized, customized, printed-circuit board size electronic solutions before the entire sensor can be packaged into a small, handheld instrument. In the interest of focusing our efforts on integrating nanowire and biological sensing into the stack we shifted our efforts away from an overall small sensor device.

### Development of a micropump module to the fluidic stack

In past efforts CAMD researchers jointly with partners at AMRI/UNO have optimized the design and fabrication of customized fluidic stacks. However, the current solution is far from perfect due to relatively big peripheral equipment such as syringe pumps which do not allow good local control of fluid flow conditions because of large dead volumes. Size is also an

obstacle for realization of fully miniaturized micro-total analysis system ( $\mu$ TASs) and lab-on-a-chip (LOCs) devices, and we have therefore started to design a pumping module compatible with the fluidic stack - the multi-fluidic-speed-modulating micropump (MSM-micropump). Fig. 7 shows the concept of adding a pump module to the fluidic stack assembly.

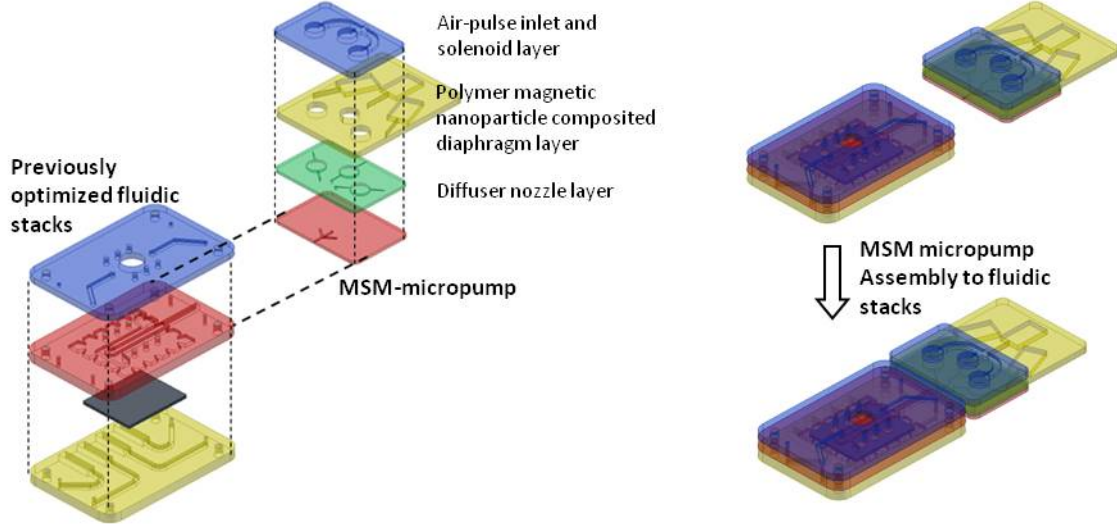


Fig. 7: left: Microfluidic biosensor chip and MSM-micropump illustrated layer-by-layer, right: assembled MSM-micropump platform mounted to the microfluidic biosensor stack.

The MSM-micropump is a membrane pump. The basic components of this pump illustrated in Fig. 8 are diaphragms, drivers or actuators, and diffuser/nozzle chamber. As described in more detail in our quarterly reports the multi-fluidic-speed-modulating micropump (MSM-micropump) is driven by one external source (oscillating compressed air) and offers local, electrical control of the fluid flow using an embedded solenoid and magnetic force exerted onto the diaphragm. The diaphragm is made from a polymer filled with magnetic nanoparticles which can be preloaded using an external magnetic field generated by a solenoid operating against a certain external air pressure (pulsed) applied via the hole of the air-pulse inlet layer. During micropump operation, the air pressure acts on the diaphragm to decrease and flatten periodically the chamber volume pushing fluid out of the chamber or drawing it into it. Flow control is realized via the valve-less nozzle and diffuser structures which are connected to the inlet and outlet of the chamber to rectify the flow. The flow rate can be controlled by solenoid magnetic force acting upon the magnetic nanoparticles filled polymer diaphragm.



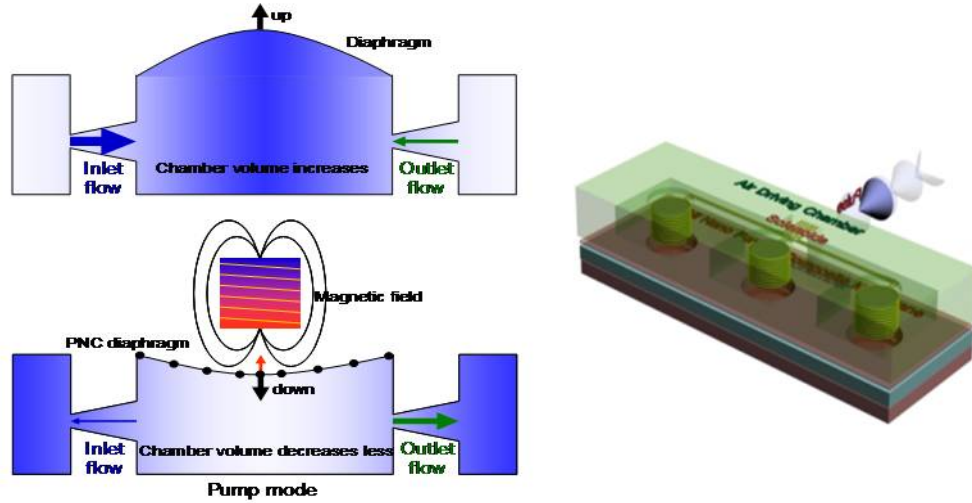


Fig. 8: Concept of operation of the MSM-micropump, left: preloading of diaphragm using an external magnetic field exerting a force onto the magnetic nanoparticles embedded in the membrane; right: assembled pump module with three pumps to regulate flow in a hydrodynamic focusing test structure.

Simulation helped with better understanding the relationship of design parameters and pump performance. In our simulation the diaphragm was actuated assuming a certain external force and calculating the correlated displacement. In addition, the magnetic force between solenoid and nanoparticles filled polymer diaphragm was calculated for a range of characteristic displacements (see Fig. 9).

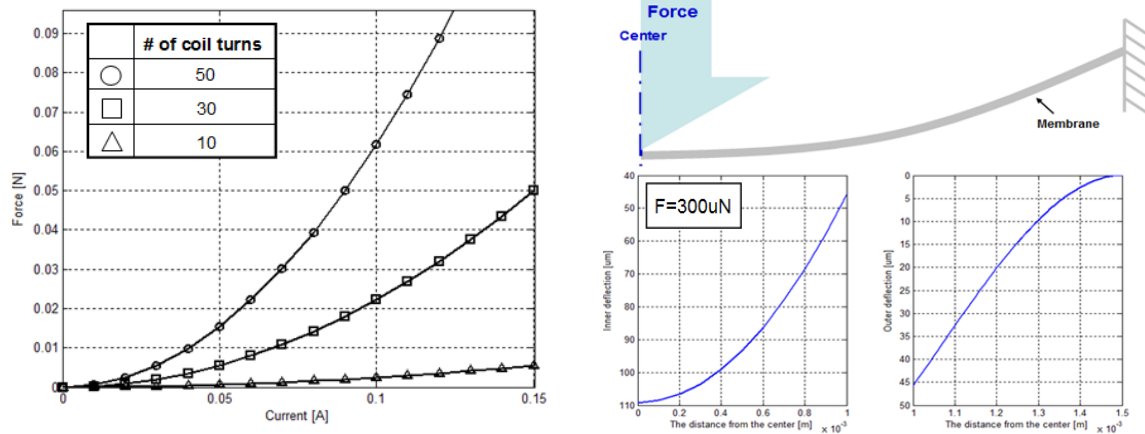


Fig. 9: Solenoids magnetic force by specifications of current, sizes, and number of turns; and a Nano particle composited diaphragm displacement by the driving force.

Given these numbers simulation of the flow rate is calculated around  $10\mu\text{m}/\text{min}$  when the solenoids are turned off and much less for preloaded diaphragms.

The diaphragm was made from PDMS loaded with Ni-nanoparticles. Diaphragms were formed by mixing the particles into the liquid PDMS and spin-coating uniform layers of the composite material onto glass or polymer substrates preconditioned with a plasma treatment (100mW RF, Oxygen, 1 min) for improved bonding. Fig. 10 shows the diaphragm thickness as a function of

spin speed for diaphragms with different Ni nanoparticles content. The optical micrographs show that the particles are uniformly mixed into the diaphragm ensuring a predictable operation.

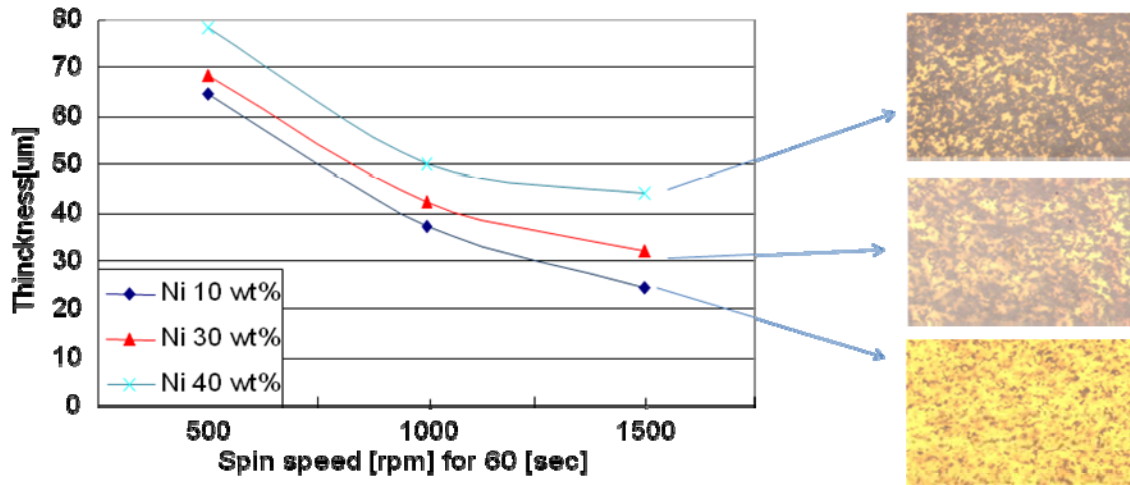


Fig. 10: PDMS-Ni diaphragm thickness as a function of spinning speed for three samples of different Ni particle weights and optical micrographs of Ni nanoparticles in the composite diaphragm.

Diaphragm operation was visualized using the setup shown in Fig. 11a. The diaphragm was bonded to a pre-structured PMMA chip and upon applying air pressure the diaphragm was stretched and a focused light beam was deflected accordingly monitored with a CCD camera (Fig. 11b).

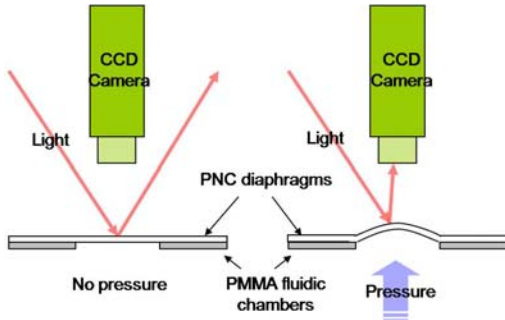


Fig. 11a: Experimental setup for monitoring membrane deflection.

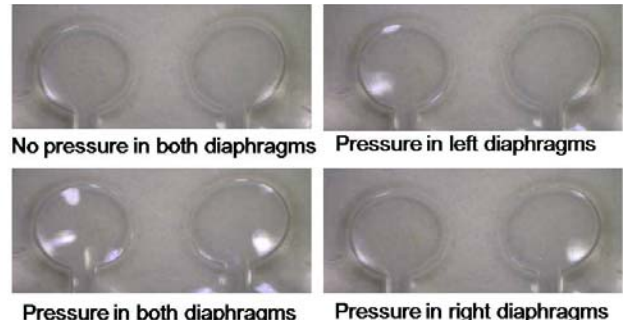


Fig. 11b: Observation of deflection indicated by a bright spot on the actuated membrane.

These initial tests demonstrate successful fabrication of diaphragms and their suitability as actuator for a micropump.

Fabrication has started by designing the bottom chamber layer including inlet/outlet. MSM-micropump design was drawn in AutoCAD considering the simulation results (Fig. 12). Several possible designs meeting different pumping requirements have been realized including changes of chamber size and channel width. Initially, a simple nozzle/diffuser was used in the simulation as fixed geometry valve. Supported by literature study it was decided to

use more complex Tesla valves instead promising a better performance. As a result, the prototype design chip size was a little larger than the standard fluidic stack chip.

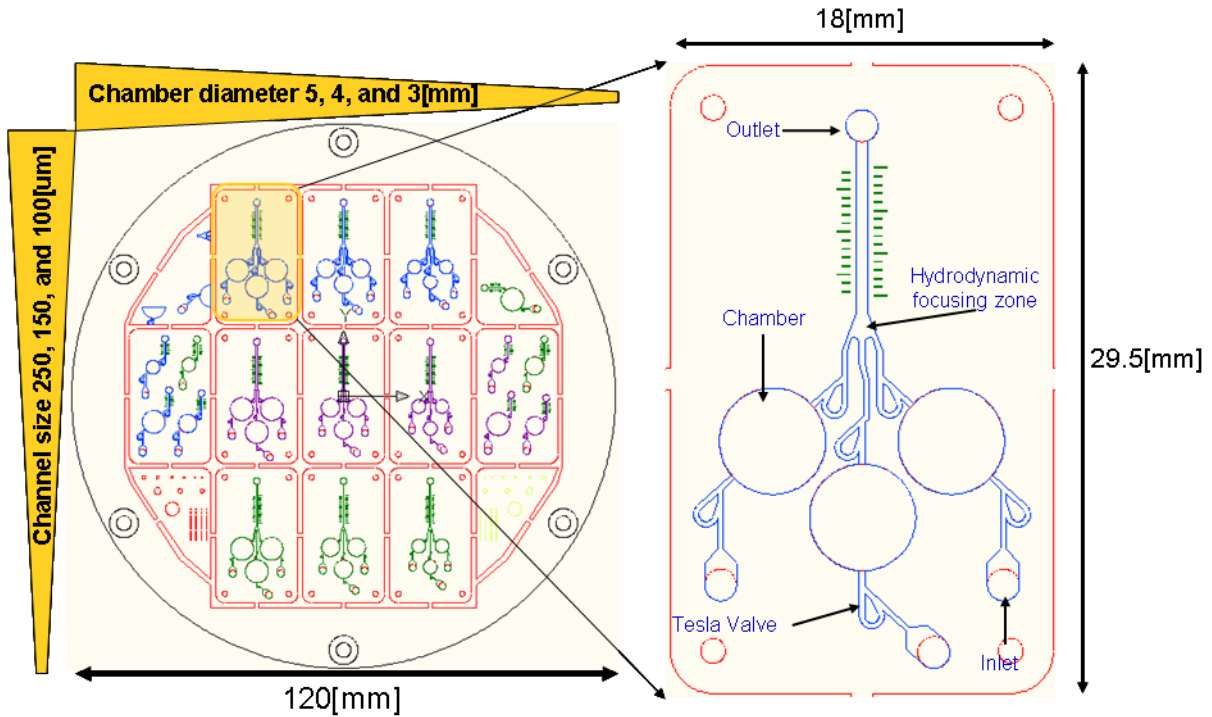


Fig. 12: MSM-micropump - AutoCAD design with variations in channel size and chamber diameter.

Precision micromilling was employed to fabricate a brass mold insert from the AUTOCAD design. Though this process is well-suited for rapid prototyping the use of drill tools with finite size and aspect ratio is limiting the quality of some structure details. Nevertheless it's appropriate for first tests and can be replaced later by a lithography-based LIGA mold insert if needed. The first generation MSM-pump mold insert is shown in Fig. 13.

Using hot embossing the insert pattern was transferred into a PMMA sheet. The different process steps are illustrated in Fig. 14. Initial tests used 1.8 mm thick PMMA sheets and a molding temperature of about 160°C. Further improvement is necessary as not all details were transferred accurately and also the molded parts showed some thermal stress/warping making the assembly difficult/nearly impossible.

Due to equipment failure (precision milling machine was done for about 2 months) the fabrication of a first pump prototype is behind schedule and results of its performance as well as suggestion for further improvement will reported in the coming quarterly reports.



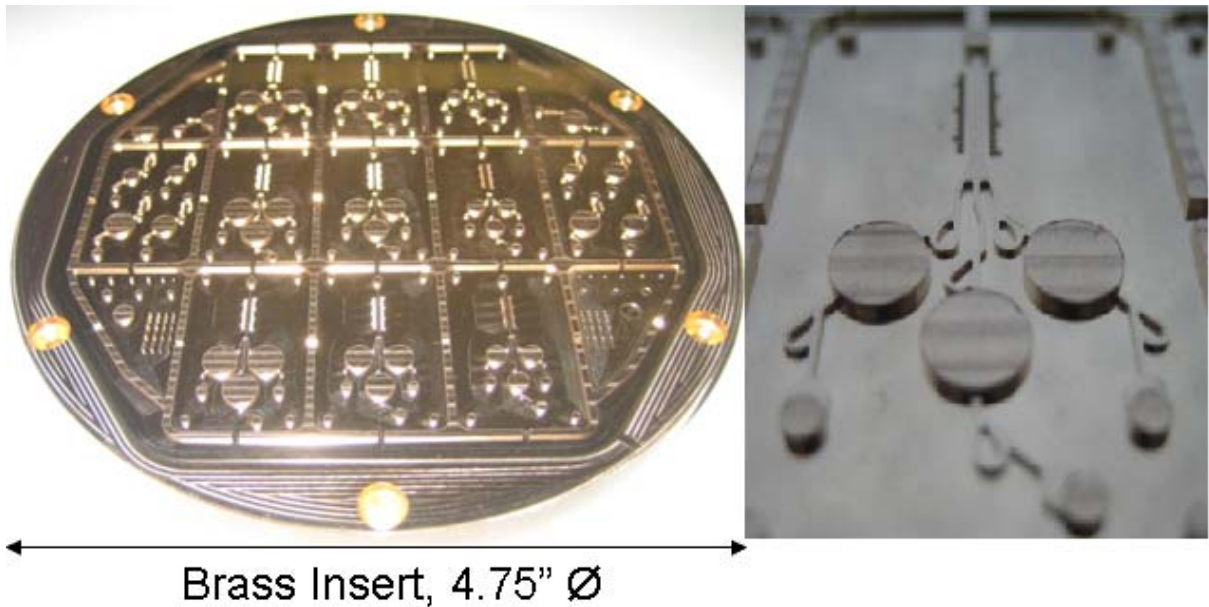


Fig. 13: MSM micropump brass mold after the mechanical micromilling.

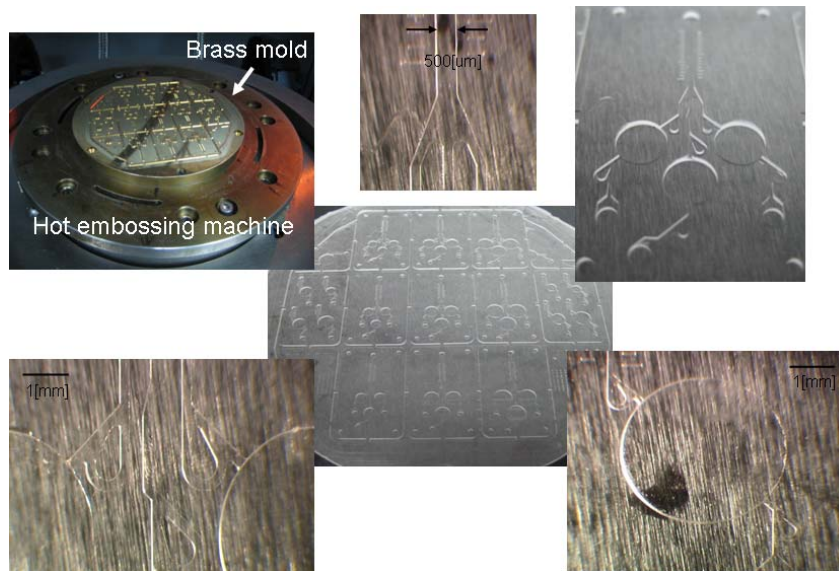


Fig. 14: PMMA chip of MSM-micropump after hot embossing process.

#### **Publications:**

N. Frische, P. Datta, J. Goettert, “Development of a biological detection platform utilizing a modular microfluidic stack”, *Microsyst Technol* online article March 2010, DOI 10.1007/s00542-010-1066-0.

P. Datta, G. George, S. Tiwari, J. Goettert; “Monolithic fabrication of electro-fluidic polymer microchips”, *Microsyst Technol* (**2009**) 15:463–469.

### **Conference Presentation**

P. Datta, M.A. Witek, M. Hupert, S.A. Soper, J. Goettert; “Bacterial Species Detection in Whole Blood Using a Modular Microfluidic System”, Proc. HARMST 2009, Saskatoon, Canada (**2009**), 245-246.

N. Frische, P. Datta, Y. Jin, J. Goettert; “Development of a Biological Detection System Utilizing the Modular Microfluidic Stack”, Proc. HARMST 2009, Saskatoon, Canada (**2009**), 195-196.

P. Datta, J. Goettert; “Multi-level Modular Polymer Microfluidics with Optimized Form Factor”, Proc. HARMST 2009, Saskatoon, Canada (**2009**), 147-148.

O. Jinka, H. Wagemanns, J. Goettert, V. Singh; “Combinatorial Multi-level Mold Inserts Using X-ray Lithography”, Proc. HARMST 2009, Saskatoon, Canada (**2009**), 109-110.

Y. Jin, K.-N. Kang, P. Datta, J. Goettert, Z.-M. Zeng, W. Zhou; “Nanoimprinting Mold with Multi-level, High- Aspect-Ratio LIGA Microstructures“, Proc. HARMST 2009, Saskatoon, Canada (**2009**), 73-74.

**Children's Hospital:**  
**co-PI: Seth H. Pincus, M.D.**

## **Project Name: Genetically engineered antibodies for nanosensors**

### **1. Brief Narrative:**

We are making genetically engineered antibodies (Abs) that will bind to nanomaterials better than the native antibodies. Working with two different antibodies we have introduced three different C-terminal domains onto them, and expressed them as full length Abs or Fab fragments. The bound antibody retains function and antigenic specificity. We have now tested the binding of these Abs to quantum dots (QDs) coated with polyethyleneglycol (QDots, Invitrogen), mercapto-undecanoic acid, and dendrons. We have attached Abs by chelation and by chemical coupling (EDC/NHS). We have now demonstrated that an engineered Ab with a 6X-His tail binds to QDs significantly better than does the parental Ab. Quantitative data suggests that another modification (oligo-lysine tail) may enhance coupling efficiency by EDC/NHS. Designing Abs specifically for binding to QDs will aid in the development of fluorescence-based biosensors.

### **2. Objectives:**

We are making genetic modifications to antibodies to improve their utility in biosensors. These modifications allow for greater coupling efficiency and for orientation of the antibodies with their binding sites exposed. Two different antibodies are being modified: 1. RAC18, an antibody to ricin toxin, a molecule of biodefense interest, and 2. anti-HIV antibody HY, a neutralizing Ab directed to the virus envelope. For each antibody, we are attaching to the full length and Fab three different heavy chain carboxy-termini: 1. the metal binding 6X-His motif, 2. oligo-lysine (free amino groups), and 3. oligo-cysteine (sulfhydryl groups). We compare the function of these 12 constructs with native Ig. They will be studied free in solution and bound to nanowires and QDs. We have made all four 6XHis constructs, and the four full-length oligo-lysine and oligo-cysteine constructs. Antibodies for each have been made and purified. We are conducting tests of the coupling of these antibodies to QDs. Our studies of the binding of these molecules to nanowires have been delayed because the chemical modification of the nanowires has not been completed. We demonstrate promising results showing the function of 6X-his and 3X (Cys, Ala) modified antibodies when attached to QDs.

### **3. Research Progress:**

Over the past year the following progress has been made.

Initial research progress was limited by difficulties in expressing the recombinant antibodies. Two problems contributed to this issue.

**Problem 1: DNA quality.** Because we are using transient expression protocols that require transfection of the DNA encoding the recombinant constructs, quantity of antibody produced is highly dependent upon transfection efficiency, which in turn is dependent upon the quality of the DNA. We now take measures to avoid contaminating our DNA with endotoxin, and to use specific kits to remove the endotoxin. We have found that Ab yields have approximately doubled as a result.

**Problem 2: Plasmids with inserts reversed.** Much to our chagrin we discovered that some plasmids that were making no antibody upon transfection had the insert, encoding the antibody, in the reverse orientation. This was found to be due to a methylated restriction site resulting in cutting within a shuttle plasmid and the resulting insert ligating into the opposite orientation. Once this was discovered, the mistake was corrected, and good yields of antibody are now being obtained. Having solved these problems, we have made 3-4 mg of each of the 6X-His ricin antibodies: native chRAC-18 IgG, 6X-His-RAC-18 IgG, and 6X-His-RAC-18 Fab.

Genetically engineered antibodies with 6X-His and 3x (Cys, Ala) tails have been compared to the parental antibodies for binding to QDs, and antibody function when bound to the QDs. Two different forms of QDs were first used: CdSe/ZnS nanocrystals surface functionalized with mercapto-undecanoic acid (termed nanocrystals, NC) or commercially available encapsulated QDs, with an amine-derivatized polyethylene glycol shell (termed QDots™) to which the antibodies are conjugated using free sulfhydryl groups using the hetero-bifunctional crosslinker SMCC. The function of these antibodies has then been studied by immunofluorescence on either HeLa cells (figures 1 and 2) by confocal microscopy, or on H9 cells, by flow cytometry (figures 3-6). The antibodies used bind to ricin, a toxin of biodefense importance. Cells were either pretreated with ricin, or as a negative control, not treated.

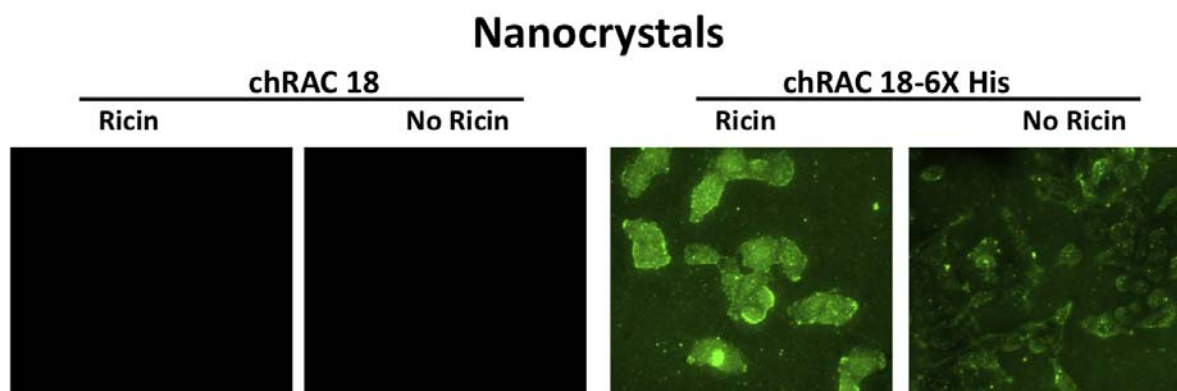


**Figure 1. Binding of antibody-derivatized nanocrystals to HeLa cells.** NCs were conjugated to parental or 6X-His antibodies in the presence of bovine serum albumin. Adherent HeLa cells were treated with ricin 10µg/ml for 1 hour, washed twice and incubated with the conjugated NCs at 10 µg/ml. There is background staining seen as ricin adhered to the slide, and a small amount of aggregates formed in the solution. But it is clear that the genetically modified antibody bound to the NCs, whereas the parental did not.

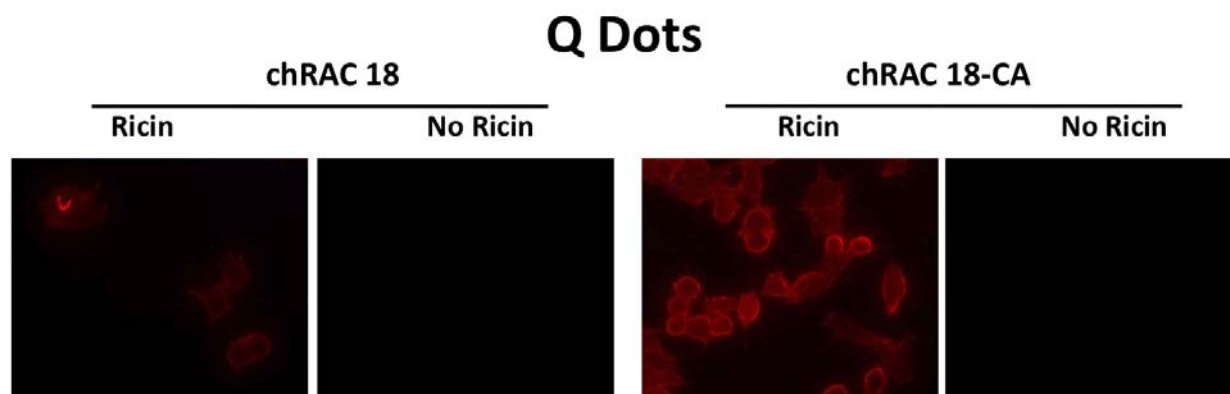


**Figure 2. Binding of antibody-derivatized QDots to HeLa cells.** Antibodies were conjugated to QDots using SMCC. Cells were treated with ricin and antibody as described in figure 1. Note that binding of the CA antibody appears to be greater than that of the parental antibody. Micrographs were taken at identical exposures.

### Binding of Nanocrystal-Conjugated Antibodies to Cells

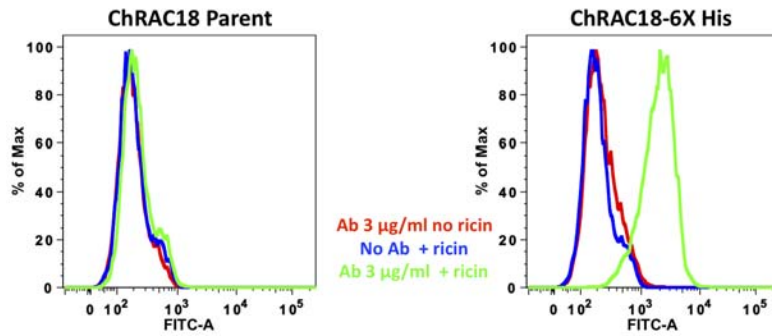


**Figure 3. Binding of NC-conjugated antibodies to H9 cells.** Nonadherent cells were treated with ricin, or not, as described above and then incubated with antibody-NC conjugates at the indicated concentration, and examined by flow cytometry. As compared to figure 1, note the lack of non-specific binding at a lower antibody concentration.

### Binding of QDot-Conjugated Antibodies to Cells

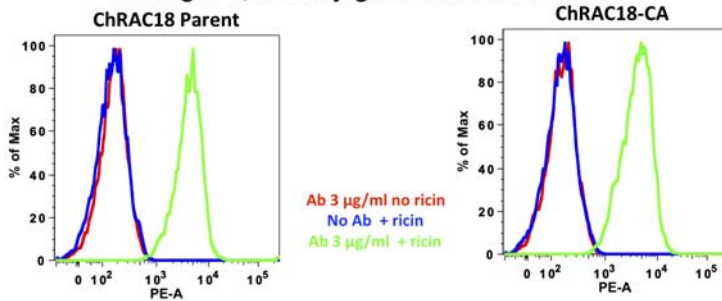


**Figure 4. Binding of QDot-conjugated antibodies to H9 cells.** The experiment was performed as in figure 3. Note that the data do not indicated greater binding by the engineered antibody, in contrast to figure 2.

### Binding of QD-Labeled Antibodies to Ricin-Treated Cells

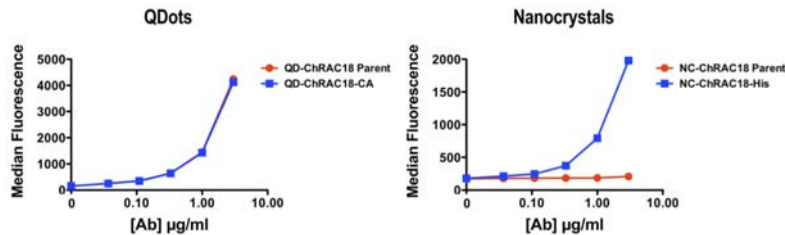


**Figure 5. Comparative titration of QD conjugated antibodies to ricin coated cells.** The experiment was performed as in figures 3 and 4, but with different concentrations of antibody-conjugated QDs. The results are median fluorescence. The curves confirm the results of figure 3 and 4.

### Relevance of Narrower Emission Spectra of Quantum Dots

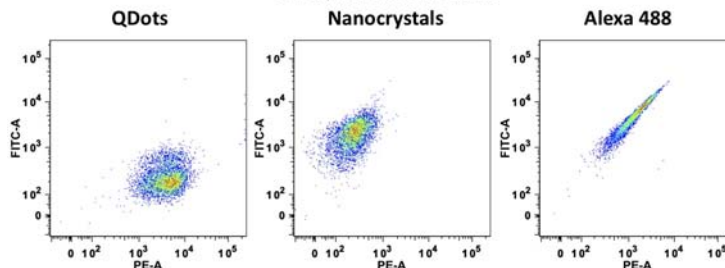


**Figure 6. Bleed through of dyes from one fluorescent channel to another.** Cells were stained as in figures 3-5 and analyzed by flow cytometry in 2 different fluorescent channels. Note that QDs fluoresce in only one channel, while the popular fluorescent dye Alexa-488 fluoresces in both.

We next focused on using our engineered anti-ricin antibodies to test a new generation of QDs, with greater stability in physiological salt solutions. The latest of these nanocrystals are coated with dendrons which have exposed COOH groups. We have compared different methods of attachment, including chelation and direct conjugation via NHS/EDC. Genetically engineered antibodies with 6X-His and 3x (Cys, Ala) tails have been compared to the parental antibodies. We have used flow cytometry to quantify the degree of binding. We have used two color confocal microscopy to track the ability of the nanocrystal labeled antibodies to remain attached as labeled-ricin moves through the cell. These studies demonstrate that dendron-coated nanocrystals have excellent binding capacity and are sufficiently small that they traffic through

Figure 7 shows flow cytometry results, where nanocrystal-antibody conjugates are incubated with cells following exposure (or not) of the cell to ricin. The results show that the LR nanocrystals give greater

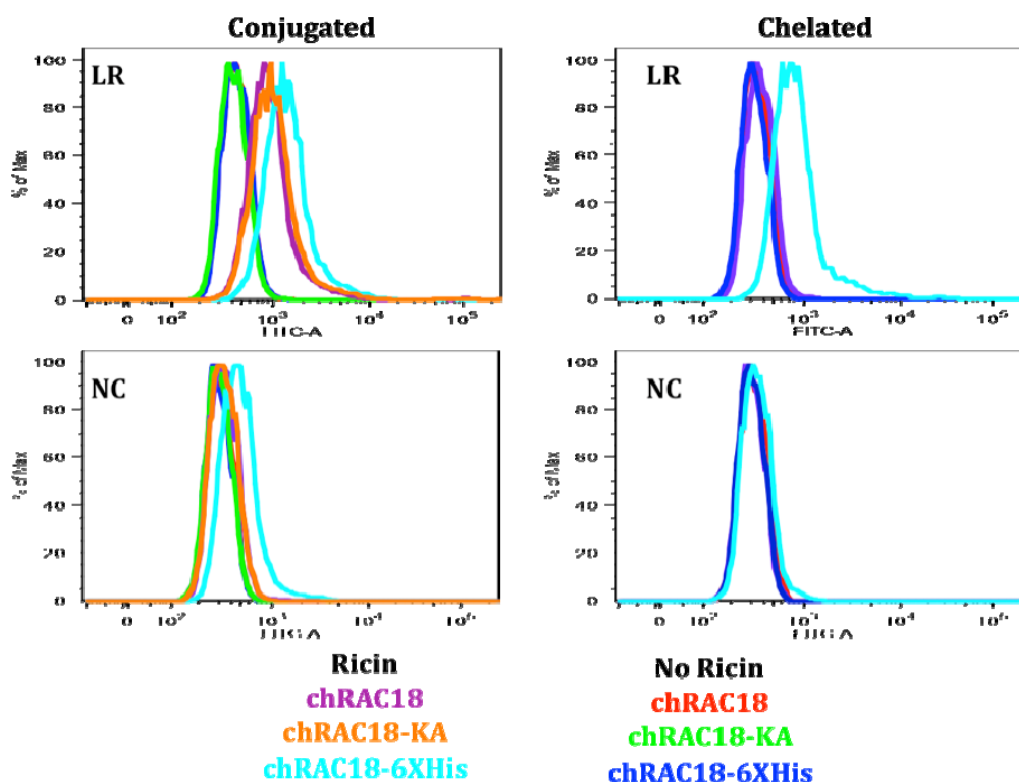


**Figure 7. Binding of antibody-conjugated nanocrystals to cells coated with antigen (ricin) as measured by flow cytometry.** Cells were incubated, or not, with ricin, washed, and then incubated with antibody-coupled nanocrystals. After a final wash, fluorescence was measured.

binding than the conventional nanocrystals (NC). The left hand panels compare the three mabs (parent, 6X-His, KA) conjugated to the dendrons using EDC/NHS; in the right hand panels the antibody is simply mixed with the NCs and binds by chelation. The results show that there is no binding in the absence of ricin. The LR nanocrystals give better results than the conventional nanocrystals. The 6XHis antibody functions best in all cases. The parental and KA antibody can also be conjugated to the LR nanocrystals, but only the 6XHis works when mixed (ie binds by chelation).



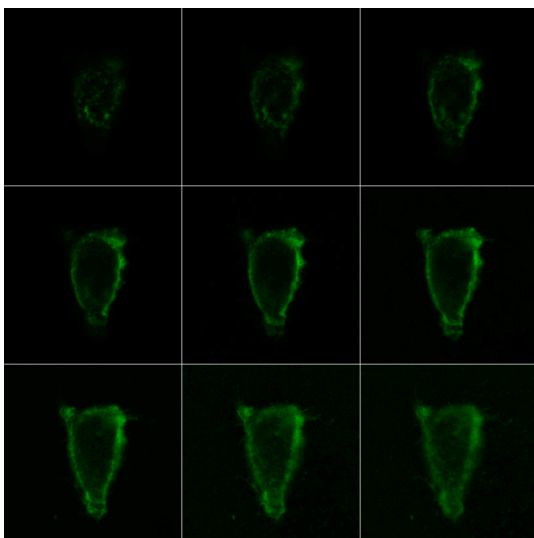


**Figure 8. Confocal Z-stack of AB-conjugated LR nanocrystals binding to a ricin coated cell.** Fluorescent images are collected at 0.5 $\mu$  intervals.

Figure 8 shows that antibodies can bind to cell-surface ricin on ricin treated cells. The cells are fixed prior to binding ricin or the antibody. Figure 9 demonstrate the trafficking of both ricin (labeled with Alexa-594) and anti-ricin antibody conjugated to LR nanocrystals, in live cells. The cells were incubated at 37 degrees with ricin and antibody for 120 minutes. Cells were fixed and then studied by confocal microscopy. Figure 9 shows 1 $\mu$  z-sections through the cells, showing each channel (Ab, ricin, DIC) individually and merged. The data show that the LR-nanocrystals can enter the cells. Interestingly, the area of least antibody binding is found at the outer margins of the cell.

Our studies have continued using flow cytometry and confocal microscopy to study binding of Abs to different QDs, each somewhat sophisticated than the last. The use of dendromer coatings has essentially solved the problem of QD stability in salt solution, while still retaining a much smaller size than PEG-coated QDots. Results of these experiments are provided in the appendix.

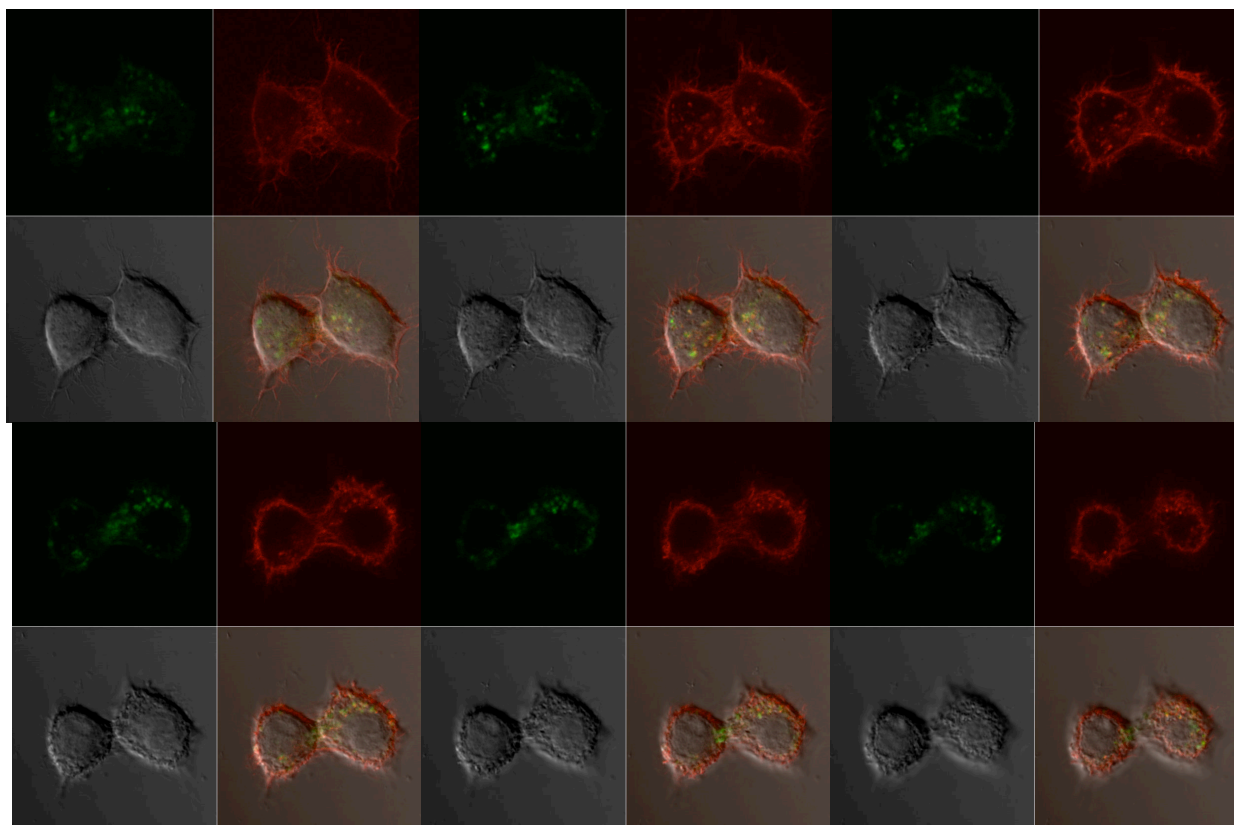


**Figure 9. Z-Stack taken of cells incubated with ricin-Alexa-594 (red) and LR-nanocrystal-conjugated chRAC18-KA (green).** Cells were incubated with ricin and Ab for 120 min. Z sections were taken in red, green, and DIC channels at 1  $\mu$  intervals. The slice at the top left are at the cell base. Slices move up as the photos go across and then down.

## LA Tech:

**Project 3: Dr. DeCoster.** To develop highly sensitive nanowire based biochips for the fast detection of secreted phospholipase A<sub>2</sub> (sPLA<sub>2</sub>) enzyme, including cell based sensors that will detect the release of stress-response molecules from living cells in situ.

1) We are using normal brain cells (astrocytes) and brain tumor cells (CRL 2199 and CRL 2020s) to evaluate the biocompatibility/toxicity of nanomaterials towards cells. Below in Figure 1 we show extensive evaluation of Silicon hollow shell/magnetic core nanoparticles provided by UNO (Zhou) compared to copper nanoparticles. Silica nanomaterials have little or no toxicity, while copper is very toxic. These results provide valuable foundation for comparing tailored materials for cell applications such as sensors and drug delivery.

## Results for Copper and Silica coated Iron

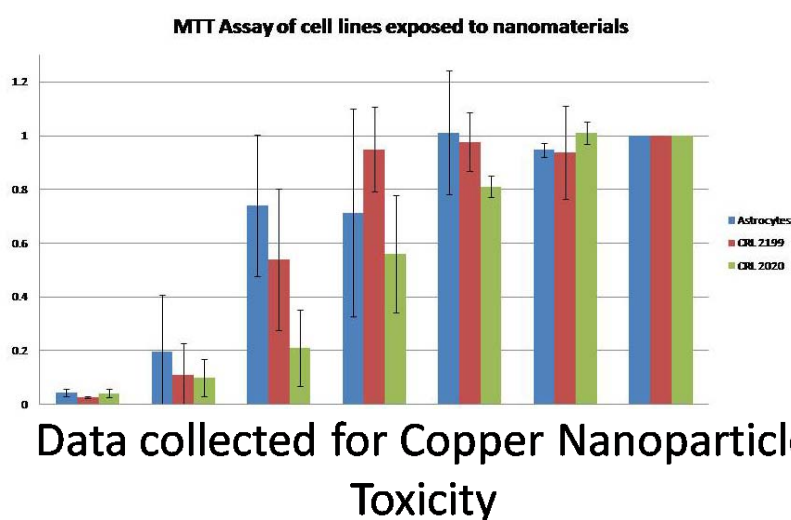


Figure 1: Comparison of toxicity of copper and hollow shell/magnetic core nanoparticles (Si) against normal brain cells (astrocytes) and brain tumor cells (CRL 2199 and CRL 2020).

For a given compound we need to calculate the half-maximal Lethal Dose (LD50). This indicates the concentration at which half of the cells are killed by the compound. By calculating the LD50 for a given compound, we can compare how toxicity of the compound varies for different cell types, in this case, normal brain cells (astrocytes and brain microvascular endothelial cells) vs. brain tumor cells. The results for this evaluation for copper nanoparticles is shown below in Figure 2.

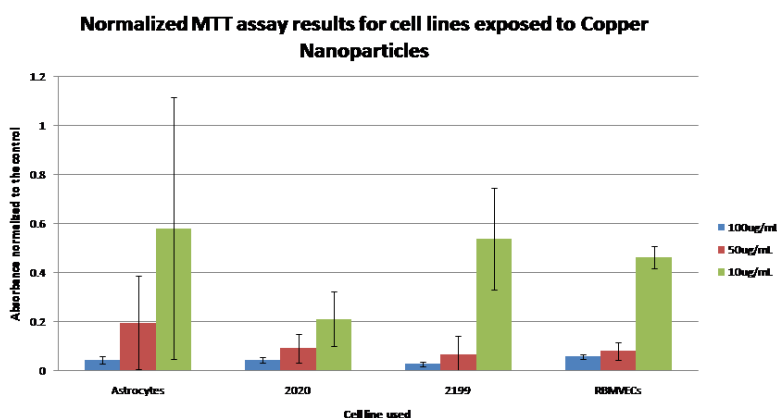


Figure 2: Comparison of copper nanoparticle toxicity across different concentrations for 4 different cell types. Astrocytes and rat brain microvascular endothelial cells (RBMVECs) are normal brain cells and 2020 and 2199 cells are brain tumor cells.

From the graphical data shown in Figure 2 above, we can calculate the LD50 values for these cells for

copper nanoparticles. The results of this analysis are shown below in Table 1.



## LD 50 of Copper NP in varying cell lines

Cell line	Estimated LD 50
Astrocyte	12ug/mL
CRL 2020	5ug/mL
CRL 2199	10ug/mL
RBMVECs	9ug/mL

Table 1: LD50 estimation of Copper Nanoparticle (NP) toxicity towards different normal brain cells (astrocytes and RBMVECs) and brain tumor cells (CRL 2020 and CRL 2199). Exposure to nanoparticles was for 21 hours before assay. RBMVECs= rat brain microvascular endothelial cells.

We have developed a protocol to determine the cytotoxicity of nanomaterials *in vitro*. This protocol is designed to be able to run quickly and be easily repeatable. The protocol is an

MTT assay, which is used for the final measurement of cytotoxicity. This protocol is currently being used to assess a wide range on nanomaterials with a variety of cells lines. The majority of the present research deals with the central nervous system. Results from these experiments are helping establish trends between different types of nanomaterials and their current state. One set of nanomaterial that we are currently using was developed by the University of New Orleans. Others are available for purchase through chemical distributors. Nanomaterials range in composition as well as reactivity. Some of the materials being used include copper, oxidized copper, oxidized iron, an iron-copper hybrid, carbon coated cobalt, and oxidized cobalt. Different cell lines are also being used to test cytotoxicity for various cell lines found around the central nervous system. Some of these include cancer lines, while others are normal type. Some cell lines have shown to be more sensitive than others to certain nanoparticles.

Nanomaterials and cellular interaction with these materials has been the focus. We have used multiple neural cell lines in this research, and both cancerous and normal cells have been utilized. The lines used were ATCC supplied CRL 2020 - human glioma, CRL 2303- rat glioma, CRL 2199- rat glioma, CRL 2570 human T-lymphoma, and Lonza supplied astrocytes.

In coordination with Dr. Yuri Lvov's lab, we have tested the natural nanomaterial halloysite. Halloysite is a nanotubes material derived from clay that is composed of aluminum oxide and silica. Initial biocompatibility testing indicates normal cells are very tolerant, as shown here.

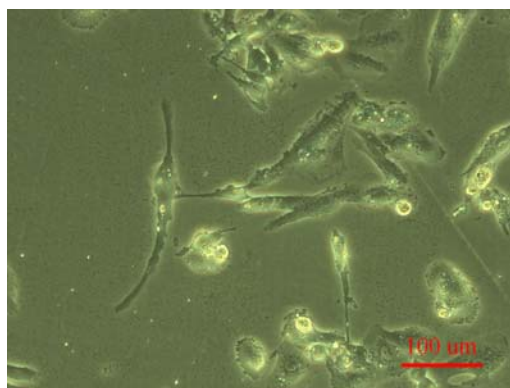


Figure 3: Normal brain glia (astrocytes) treated with 50µg/mL halloysite. Note cell clearance in immediate vicinity of membranes.

We are also looking at compatibility of Halloysite in tandem treatments with other nanomaterials. This could lead to drug delivery strategies nad cumulative treatment effects. We will begin to measure the inflammatory response of cells to halloysite, as we have

already seen that it may decrease the toxicity of copper nanoparticles. These copper nanoparticles have been used as the standard of toxicity and incompatibility in previous work (H. Ma, et al. 11/2008), but pre-treatment with halloysite seems to blunt their effects.

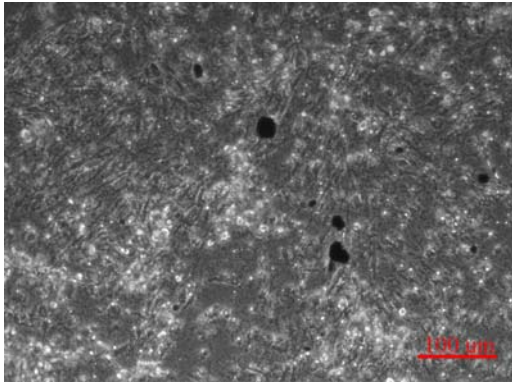


Figure 4: Astrocytes treated with 50μg/mL halloysite followed by 50μg/mL copper nps, shown here at 20 hour timepoint, cells are very obviously not dead as expected.

These findings suggest a basis for future work, along with investigations into sonication techniques that would ensure smallest particle size and fluorescent labeling of nanomaterials.

We have already received, through Dr. Lvov's lab, a sample of halloysite labeled with FITC, a fluorescent dye. We will be able to use this to show halloysite uptake into the cells with confocal microscopy. This

will lead to longer term compatibility testing, with capacity for visualizing the substance of interest, as the cell continues along the lifecycle.

Currently a protocol is being developed that can be used to determine the cytotoxicity of nanomaterials *in vitro*. This protocol is designed to be able to run quickly and be easily repeatable. Currently, an MTT assay is used for the final measurement of cytotoxicity. This protocol is currently being used to assess a wide range on nanomaterials with a variety of cell lines. The majority of the present research deals with the central nervous system. Results from these experiments are helping establish trends between different types of nanomaterials and their current state.

2) Met with focused research group 1 (FRG 1) members Drs. Zhou and Pincus in New Orleans at the annual UNO-AMRI Mardi Gras review in February 2010. Provided Dr. Zhou with annual update information for his slide presentation. Provided Dr. Zhou and his Research Associate Baobao Cao with novel nanomaterials fabricated at Louisiana Tech for transmission electron microscopy (TEM) analysis. Samples were scanned and an example of scanned sample is shown in Figure 5 below:

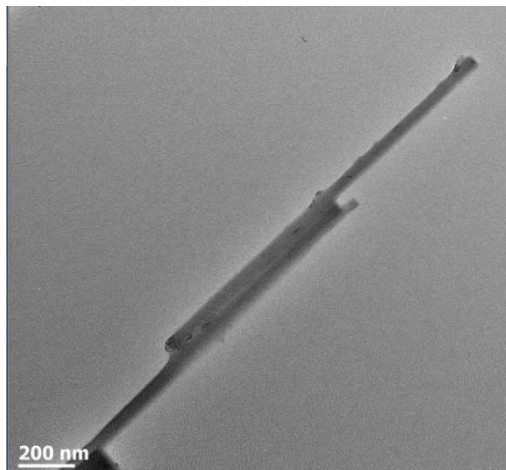


Figure 5: Transmission Electron Microscope (TEM) example image of synthesized nanostructure. Scale bar indicates 200 nanometers and demonstrates that diameter of final structures is 25 nm or less, with length in the micrometer range.

With Dr. Pincus' group discussed linking antibodies to novel linear nanostructures for development of bio-sensors. Two sets of materials were shipped to Louisiana Tech for this effort: 1) chRAC18 and chRAC18-His (6XHis) antibodies and 2) Transferrin-Alexa 594, Ricin-Alexa 594, and HY-His antibody (negative control for the chRAC-His antibodies). These reagents will be used to link antibodies to metals-based structures and then use the antibodies for biosensor detection purposes.

3) Submitted abstract to annual Society for Neuroscience (SFN) meeting describing effects of sPLA<sub>2</sub> on brain tumor cells (see below). Submitted white paper proposal to utilize novel nanomaterials for oil spill remediation. In collaboration with Dr. Lvov utilized nanoenabler instrumentation to print adhesive proteins and trap charged micro- and nano-capsules for developing better drug delivery and biochip development (Figure 6).

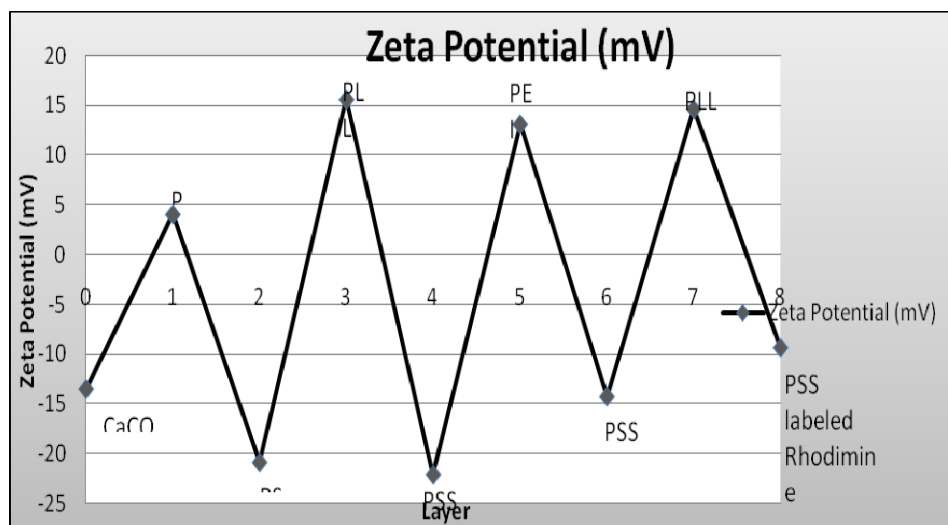


Figure 6: Zeta potential measurements were acquired by Zeta Potential Analyzer system to determine charge of capsule. As a final step capsules were labeled with rhodamine (red) for visualization.

Labelled microparticles were then trapped on a positively charged surface of PLL, labeled with Fitc (green) for visualization as shown in Figure 7.

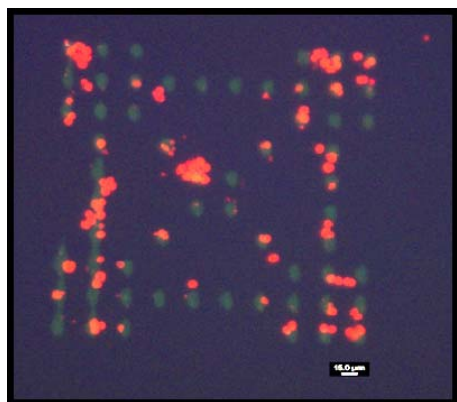


Figure 7 confocal merged image of coated microparticle attachment (red) to micropatterned nanoengineered surface (green) at 200x magnification. Scale bar= 15μms

**Personnel:** Drs. M. DeCoster, Y. Lvov D. Davis and 6 graduate students were involved (2 female) .

**Nature and Scope of Partnership Activities;** 1. Have provided Dr. W. Zhou with novel nanomaterials synthesized at Louisiana Tech for TEM scanning and have received digital images of these samples. 2. Have received antibodies, controls, and associated material from Pincus lab for linkage to metals-based nanomaterials for biosensor development. 3. Our clay nanotube samples loaded with silver were prepared for TEM study at AMRI, K. Stokes 4. Have discussed electron microscopy characterization of novel materials with Dr. W. Zhou. 5. Hollow silica shell magnetic-core nanomaterials provided by Dr. Zhou (UNO) continue to be evaluated for biocompatibility by DeCoster lab (LaTech).

**Problems encountered during the last year of project activities.** None

**Contributions:****New proposals submitted / pending:**

1. “Clay Tubule Nanocontainer for Responsive Corrosion Protection,” NSF-nanomanufacturing, PI: Lvov, \$270,000, Oct 2010- Sept 2013
2. “Halloysite Tubule Nanocontainers for Self-Healing Composites,” DoD-STTR, PI: Y. Lvov (with Luna Innovation Corp), \$90,000, July 2010-Jan 2011
3. “Substrates for Surface Enhanced Raman Scattering Sensing,” DoD-STTR, PI: Y. Lvov (with Radiance), \$90,000, July 2010-Jan 2011

**New proposals funded:**

1. “Layer-by-layer Nanocarriers for Highly Efficient [Solubilization](#) of Insoluble Drugs,” PI- Lvov, 1-R01-CA-134951-01A2, \$1,200,000 (with Northeastern University, my part \$550,000); February 1, 2010 – December 31, 2014.
2. “Nanomaterials Safety Lab: Research Integrated with Service and Education (RISE)”, DeCoster-PI, (Lvov, co-PI), Louisiana BOR enhancement proposal, \$93,244 , July 2010- June 2011.
3. “Healing Polymer Composites Based on Clay Nanotubes,” BoR NASA-LURA, \$6,000, PIs: Lvov, July 2010-May 2011

**Project Revision:** Provide a listing of and explanation for any significant changes in the work plan for upcoming year, including any changes in the amount of investigators' time devoted to the project. – none

**Work Products:** List any tangible products (e.g., research publications and/or presentations, etc.). Please combine all products into one document.

**National conference organizing:**

Y. Lvov is appointed as an organizer and chair of International Symposium “Clay / Polymer Nanocomposites: from Nanoplates to Nanotubes” at 241<sup>st</sup> National Meeting of American Chemical Society, PMSE-Division, Anaheim, CA, March 27-30, 2011.

**National funding agency review panel:**

M. DeCoster, serving on NIH R03 cancer prevention study section (June 2010).

**Peer reviewed papers / published:**

1. R. Bellamkonda; [T. John](#); B. Mathew; M. DeCoster; H. Hegab; [J. Palmer](#); [D. Davis](#), **Proceedings of SPIE- The International Society for Optical Engineering** V. 7318, 2009, Article number 73181H, “Microfabrication of nanowires-based GMR biosensor”.
2. E. Abdullayev, R. Price, Y. Lvov, **ACS Applied Materials & Interfaces**, v.2, 1437-1442, 2009, “Halloysite Tubes as Smart Nanocontainers for Anticorrosion Agent Benzotriazole”
3. D. Fix, Y. Lvov, D. Shchukin, **Advanced Funct. Materials**, v.19, 1720-1727, 2009, “Application of Inhibitor Loaded Halloysite Nanotubes in Active Anticorrosive Coatings”
4. V. Vergaro, E. Abdullayev, R. Cingolani, Y. Lvov, S. Leporatti, **Biomacromolecules**, v.11, 820-828, 2010, “Cito/biocompatibility and Uptake for Clay Nanotubes,”

5. C. Yelleswarapu, E. Abdullayev, Y. Lvov, D. Rao, **Optics Commun.**, v.283, 438-441, 2010 "Nonlinear Optics of Nontoxic Nanotubes"
6. Bellamkonda, R., John, T., Mathew, B., DeCoster, M.A., Hegab, H., Davis, D. "Fabrication and testing of a CoNiCu/ Cu CPP-GMR nanowire-based microfluidic biosensor." **J. Micromech. Microeng.** v.20, #025012, 2010
7. R. Mannam, M. Agarwal, A. Roy, V. Singh, K. Varahramyan, D. Davis, "Electrodeposition and Thermoelectric Characterization of Bismuth Telluride Nanowires" **J. Electrochemical Society**, v.156, B871-B875, 2009.

#### **Presentations:**

1. M. A. DeCoster, J. McNamara, K. Cotton, R. Masvekar, "Delay of staurosporine-induced apoptosis by glutamate in brain tumor glia and normal astrocytes" Society for Neuroscience Meeting, Chicago, October 20, 2009.
2. R. Masvekar, J. McNamara, X. Du, A. Kunjumon, D. Green, S. Dua, D. Davis, M. DeCoster "Glial Cell Interfaces: Using Micro- and Nano-patterning for Brain Tumor Studies" American Soc. Cell Biology/ RIKEN joint meeting: "Building the Body Plan: How Cell Adhesion, Signaling, and Cytoskeletal Regulation Shape Morphogenesis.", Kyoto Japan, September 22, 2009.
3. M. DeCoster, "Neurotoxicity of Nanoparticles", South Central Society of Toxicology (SCST), Annual Fall Meeting October 8-9, 2009 Shreveport, LA.
4. Y. Lvov, R. Price, E. Abdullayev, "Halloysite- benzotriazole nanocomposites, low cost additive to metallic coatings for corrosion protection," 29<sup>th</sup> Biennial Western Coating Symposium, Las Vegas, NM, October 25-28, 2009

#### **Report of Inventions:**

1. DeCoster, M. and Wasserman, J.: "Biological production of ordered XXXX structures from nanoparticles". Filed with Louisiana Tech University, ROI #2009-17.
2. D. Mills, Y. Lvov, "Smart Bioactive Nanocoating with Sustained Drug Release Capability for Implants, Wound Repair and Tissue Regeneration," April 23, ROI #2010-08
3. Y. Lvov, "Selective Hydrocarbon Grafting of Halloysite Lumen to Produce Inorganic Micelle-like Petroleum Sorbent Material," May 14, ROI #2010-12

John Wiley  
(PKSFI FRG-2, 2009-2010)

FRG-2 Nanomechanical Devices

1. Personnel:

This focused research group consists of researchers from the University of New Orleans (UNO) and Tulane University (TU). The principal investigators are John Wiley (UNO), Bruce Gibb (UNO), Leonard Spinu (UNO), Vijay John (TU), and Hank Ashbaugh (TU). A number of graduate students are also contributing to the work: Jianxia Zhang (UNO), Haiying Gan (UNO), Andrei Diaconu (UNO), Joy St. Dennis (TU), Bhanu Sunkara (TU), and Piyush Wanjari (TU). In one project, photoactive polymers are being synthesized and tested as possible light and/or solvent driven actuators in mechanical devices (Zhang in Wiley's group). In another project, sets of host-guest molecules are being synthesized and characterized as possible tethers for the directed self-assembly of nanocomponents (Gan in the Gibb's group). New magnetically guided tubular liposomes have also been produced for potential mechanical device components (Joy St. Dennis and Bhanukiran Sunkara in V. John's group; these researchers are working with Leonard Spinu in the characterization of these materials). The Ashbaugh group has studying solvent effects on solvent-mediated interactions between hydrophobic species.

2. Activities and Findings:

The activities and findings will be broken up into the various aspects of the program.

- a. *Photo- and/or solvent-active polymers.* We are continuing our efforts to investigate the potential use of diazobenzene polymers for optically-active and solvent-active actuators. The polymers have been formed into nano- and micron-sized wires (Figure 2-1) and we are now studying the mobility of these object under various conditions. We can follow the movement of micron-sized wires with an optical microscope. Nanoscale wires are more of a challenge. We initially planned to carry out experiments to follow the movement with an STM, and while may still do so, we are now following a different strategy based on the insertion of quantum dots into the wires. In this case we can use a fluorescence microscope to follow the movement. In an additional part of this effort we are looking at asymmetric modification of wires prior to solvent treatment to direct the bending and spiraling of micron-sized wires. Figure 2-2 shows an example of a wire that was coated with metal on one side and then treated with solvent; the solvent caused swelling

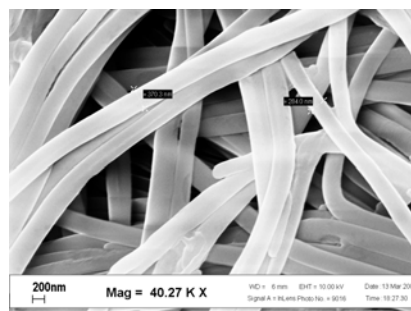


Figure 2-1. Diazobenzene wires. SEM of nanowires.



and bending of the wire component. In this case the wire curled into a spiral. We continue to examine both the effects of UV and solvent exposure on these various wires. We have a new scanning probe microscope on order that will allow us to monitor individual wires while they are exposed to UV light or different solvents.

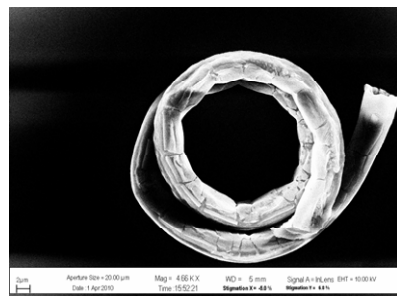


Figure 2-2. Spiral micron wire formed by swelling of asymmetrically coated surface.

- b. **Host-guest assembly.** This program of research focuses on the controlled assembly of nano-objects into complex nano-systems. The general approach involves the development of hosts (H1, H2 and H3) that bind complementary guests (G1, G2 and G3). Each host-guest pair is orthogonal, i.e. H1-G1 strongly associates, but for example H1-G2 or H3-G1 do not. Hence, one surface of a nano-object coated with H1 will stick to another object coated with G1. Moreover, with three, orthogonal host-guest pairs, it is theoretically possible to assemble complex objects by selectively coating different objects (or different parts of objects) with different hosts and guests. Our strategy is to utilize thioether-functionalized deep-cavity cavitand hosts (DCC) and complementary guests that bind strongly to gold surfaces.

Currently the student involved in this project, Haiying Gan, is focusing on the binding behavior of a series of DCC. Various binding studies involving NMR and isothermal titration calorimetry. These solution studies serve as an important foundation for working with these hosts at surfaces and interfaces.

c. **Modeling of Host-Guest systems.**

All our previous investigations provided a detailed knowledge about the hydrophobic interactions responsible for the recognition and binding of a variety of guests by the deep-cavitand hosts. We further moved towards understanding the interactions between these hydrophobic hosts, which forms capsular nanocomplexes in presence of suitable guest like adamantane. Recent experimental studies by Ramamurthy group at University of Miami indicated that neutral adamantane prefers both 2:1 and 2:2 host-guest capsuleplexes. By performing the umbrella sampling simulations combined with WHAM, we determined the potential mean

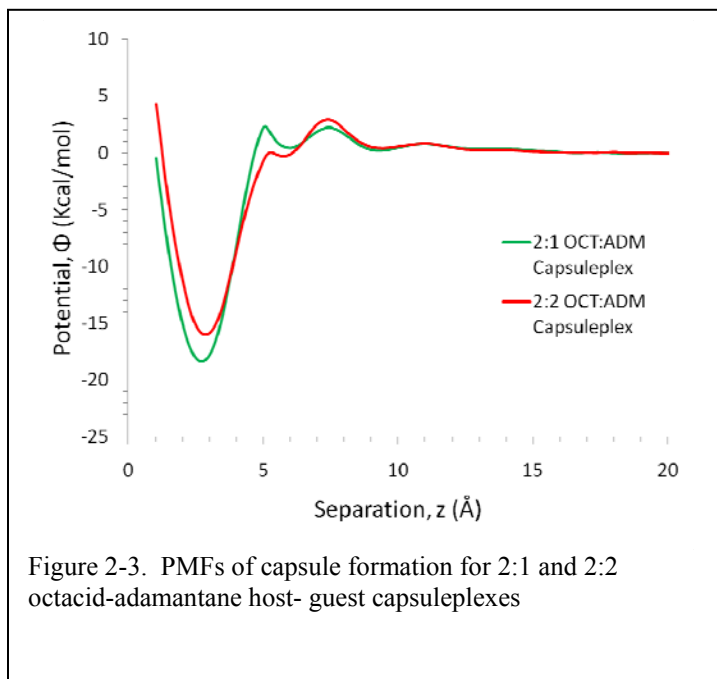


Figure 2-3. PMFs of capsule formation for 2:1 and 2:2 octacid-adamantane host- guest capsuleplexes

forces (PMFs) for both the cases by following a similar procedure that we used for the evaluation of PMF between adamantane guest and cavitand. The PMFs shown for 2:1 and 2:2

capsuleplex formation in figure 1 indicate the attractive interaction between the hosts with potential depth of  $-18.4$  and  $-16.0$  kcal/mol respectively.

Since our last reporting period, we have continued performing simulations to examine the interactions for capsule formation on the LONI supercomputer network. We have encountered issues concerning convergence of our simulation results, and are in process of simulating longer to overcome this difficulty. In addition we performed preliminary simulations to examine the free energy associated with the mutual rotation of the cavitands about their central axis. Unfortunately we found the constraints to maintain co-axial rotation were unstable and were unable to perform these calculations.

d. ***Biomimetic Nano Lubricants: Gels Based on Biomolecules and Nanoparticles with Ultralow Coefficients of Friction.***

Lubricants play an integral role in the operation of several technologies ranging from moving parts in machinery to the biolubrication of articular joints. The main purposes of a lubricant are to reduce friction and surface wear. We have found that an easily synthesized system of monodisperse hard carbon submicron spherical particles (HCS) has frictional coefficients that start approaching those of synovial fluids. When these observations are coupled with a novel discovery that a modified biopolymer (chitosan) is able to gel vesicles, we are able to realize a unique gel system containing the carbon microspheres serving as nodes in a network of this biopolymer. This forms the basis of our work to develop novel gel based lubricants containing monodisperse particles or cushioning vesicles. Our hypothesis is that these composite materials will be able to reduce friction and minimize surface wear synergistically through the boundary lubrication of biomolecules/biopolymers and the “rolling” mechanism (similar to ball bearings) employed by HCS particles. We are therefore developing biomimetic lubricants with ultralow coefficients of friction that are relatively easy to synthesize and are robust enough for applications either as potential substitutes for synovial fluid or in applications to microfluidics or microelectromechanical devices. Several formulations composed of phospholipid based liposomes, biopolymers and carbon microspheres will be explored systematically to determine the optimal molecular and particulate design that exhibits good lubrication properties including a low coefficient of friction and minimal surface wear.

### **3. Contributions:**

Initially the focus was on building the research group, attracting students, initiating the research, and building the collaborations. This is now well established. All the students supported on this grant are getting extensive training in materials research.

Some team members (John and Ashbaugh) have recently been informed that their NSF proposal relating has been approved for funding. This will leverage the PKSFI efforts. The Principal Investigator on this grant is Dr. Noshir Pesika at Tulane and both Ashbaugh and John are co-PIs.



V. John is also using carbon microsphere technology for a project on the environmental remediation of chlorinated compounds. A startup company (NanoFex LLC) has been formed based on this technology.

Further members from this team along with members of the other FRG's are initiating efforts for a center of excellence grant to the NSF. Pre-proposal submissions are due in the fall.

#### **4. Project Revision:**

Scott Whittenburg is no longer on this grant. His funds have been shifted to two assistant professors to help further their careers.

#### **5. Work Products:**

##### ***Presentations***

“Reverse Templating of Mesophase Ceramics to produce Highly Porous Structured Carbons from Sugars”, Joy St. Dennis, Vijay T. John presented at the AIChE Annual Meeting, Nashville, November 2009.

“Multifunctional Hybrid Colloidal and Nanoscale Materials for Targeted Remediation of Chlorinated Hydrocarbons”, B. Sunkara, V. John, presented at the AIChE Annual Meeting, Nashville, November 2009.

“Environmental Remediation of Chlorinated Hydrocarbons Using Multifunctional Nanoparticles with Optimal Reactive/Adsorptive/Transport Characteristics”, Vijay T. John, Jingjing Zhan and Bhanukiran Sunkara, ACS Colloid and Interface Science Symposium, Akron, June 2010.

“Hard Carbon Spheres as Micro-Bearings for Water-Based Lubrication”, Noshir Pesika, Vijay John, Joy St Dennis and Kejia Jin, ACS Colloid and Interface Science Symposium, Akron, June 2010.

“Reactions Inside and Outside Water-Soluble Nano-Capsules,” Bruce C. Gibb, University of Georgia, April **2010**.

“Reactions Inside and Outside Water-Soluble Nano-Capsules,” Bruce C. Gibb, Symposium on Self-Assembled Molecular Containers, American Chemical Society 239<sup>th</sup> National Meeting, March, **2010**.

“Magnetization Dynamics for NonVolatile Memory Technologies,” Leonard Spinu, Invited talk at the 10th International Conference on Development and Applications Systems - DAS 2010, Suceava, Romania 2010.

##### ***Publications:***

J. E. St.Dennis , Pradeep Venkataraman , Jibao He, Vijay T. John, Stephen J. Obrey, Robert P. Currier , Marisabel Lebrón-Colón , Francisco J. Sola, Michael A. Meador. “Rod-like carbon nanostructures produced by the direct pyrolysis of  $\alpha$ -cyclodextrin”, submitted to *Carbon*.

Bhanukiran Sunkara, Jingjing Zhan, Jibao He, Gary L. McPherson, Gerhard Piringer, and Vijay T. John, “Nanoscale Zero-Valent Iron supported on Uniform Carbon Microspheres for the *In situ* Remediation of Chlorinated Hydrocarbons,” submitted to *ACS Applied Materials and Interfaces*.

Zhan, J.; Sunkara, B.; Zheng, T.; McPherson, G.; Piringer, G.; Lu, Y.; Kolesnichenko, V; John, V. “Nanostructured Multifunctional Materials for Environmental Remediation of Chlorinated Hydrocarbons”, in *Environmental Application of Nanoscale and Microscale Reactive Particles*, ACS Symposium Series, K. Carvalho-Knighton, C. Geiger, Eds., 2009, 1027, 163.

“Bending Behavior of Polymer Films in Strongly Interacting Solvents,” Jianxia Zhang and John B. Wiley, *Mater. Res. Soc. Symp. Proc.* **2009**, 1129, 1129-V04-05.

“Kinetic Resolution of Constitutional Isomers via Protection by a Supramolecular Nanocapsule,” Simin Liu, Haiying Gan, Andrew T. Hermann, Steven W. Rick and Bruce C. Gibb. *Nature Chemistry*, in press.

“TTC Analysis of Guest Binding to a Deep-Cavity Cavitand,” Haiying Gan, Bruce C. Gibb, *J. Supramolecular Chem.*, submitted.

## **PKSFI Report for LEQSF(2007-12)-ENH-PKSFI-PRS-04**

**Kevin L. Stokes**  
**(PKSFI FRG-3, 2009-2010)**

### **FRG-3: Nanomaterials for Energy Conversion and Storage**

#### **1. Personnel:**

##### **LATech/IfM**

Silky Abbott, Graduate Research Assistant, Thermoelectrics  
Abdullayev, Elshad. Graduate Research Assistant, Hydrogen storage materials  
Davis, Despina. Co-PI, Thermoelectrics  
Lvov, Yuri. Co-PI, Hydrogen storage materials  
Mannam, Raja. Graduate Research Assistant, Thermoelectrics  
Wei, Wenbo. Graduate Research Assistant, Hydrogen storage materials

##### **LSU**

Haldolaarachchige, Neel. Graduate Research Assistant, Thermoelectrics  
Karki, Amar. Staff Scientist, Thermoelectrics  
Young, David P. Co-PI, Thermoelectrics

##### **UNO/AMRI**

Gabrisch, Heike. Co-PI, Battery materials  
Malkinski, Leszek. Co-PI, Ferroic composites  
Mohanty, Debasish. Graduate Research Assistant, Battery materials  
Nolting, Westly, Undergraduate Research Assistant, Thermoelectrics  
Stokes, Kevin L. Co-PI, Thermoelectrics  
Ward, Tom. Graduate Research Assistant, Ferroic composites

Dr. Kevin Stokes reviews quarterly progress reports from LSU and La Tech to ensure that these contributions meet the project's requirements.

#### **2. Activities and Findings**

##### **Major Research and Educational Activities Undertaken**

This focused research group (FRG) is applying the science and engineering of nanometer-scale materials to several areas of energy conversion and storage. Stokes, Davis and Young are investigating various aspects of nanocomposites thermoelectric materials and microdevices, Gabrisch is investigating novel electrode materials for electrochemical storage applications (rechargeable batteries); Malkinski is researching novel magnetic to electrical power conversion composites for micropower applications and Lvov is developing techniques for the nanoassembly of nanoparticles and tubule nanocontainers for possible hydrogen storage applications. There are six principle investigators, one senior researcher, seven graduate students (total) and two undergraduate students from the University of New Orleans, Louisiana State University and Louisiana Tech. The results for June 2009 to June 2010 are summarized below.

##### **Major Findings and Results**

#### **a. Giant Magnetoresistive (GMR) Sensors (Davis)**

GMR-based microfluidic biosensors are used in applications involving the detection, analysis, enumeration and characterization of magnetic nano-particles attached to biological mediums such as antibodies and DNA. Here, we introduce a novel multilayered CoNiCu/Cu nanowire GMR based microfluidic biosensor. Figure 3.1 shows the major steps in the micro-device sensor fabrication. Figure 3.1 (a) exemplifies the GMR nanowire array (magnetic sensing element material) placement on the “master” silicon wafer. The CoNiCu/Cu GMR multilayered nanowire based material has been electrodeposited in-house from a single electrolyte using a pulsed potential technique. The GMR nanowire array with electrical contacts was placed on a UV-lithographically patterned (300  $\mu\text{m}$  width, 60  $\mu\text{m}$  height and 4 cm length) silicon wafer (1  $\mu\text{m}$  oxide layer). Figure 3.1 (b) illustrates how the GMR nanowire array gets embedded in the PDMS laid to mold after the patterned silicon wafer.

PDMS is poured onto the silicon master wafer with the GMR membrane placed above of the protruding patterned mounts. The GMR electrical contacts were brought out of the PDMS and the polymer was allowed to solidify for 24 hours. Figure 3.1 (c) shows the embedded GMR nanowire array PDMS being peeled-off the master wafer and the resulting microchannels replica. Figure 3.1(d) illustrates how the micro-channel in the PDMS containing GMR was sealed using Oxygen- Reactive Ion-Exchanger (RIE) onto glass. The operating conditions used for bonding of PDMS and glass were: pressure = 700 mT, power = 20 W and time = 30 s. Figure 3.1 (e) reveals a schematic of the final device ready for testing. Tygon tubing was secured by epoxy into the previously drilled glass holes. Figure 3.2 shows a schematic of the sensor testing mechanism.

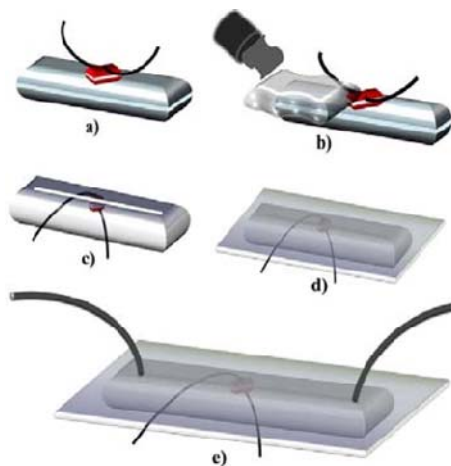


**Figure 3- 1. Sensor Microfabrication Schematic a) GMR nanowire array with electrical contacts, b) PDMS coverage of the nanowire array (sensing element) on positively patterned silicon wafer, c) Peeled off PDMS mold with open channel, d) Glass sealed GMR-PDMS channel mold, e) Final GMR microfluidic device with attached tygon tubing.**

The CoNiCu/Cu multilayered nanowire GMR based microfluidic sensor was tested potentiostatically using a computer controlled function generator (Solatron, SI 1287). A syringe pump was used to control the flow of various magnetic and non-magnetic fluids through the microchannel.

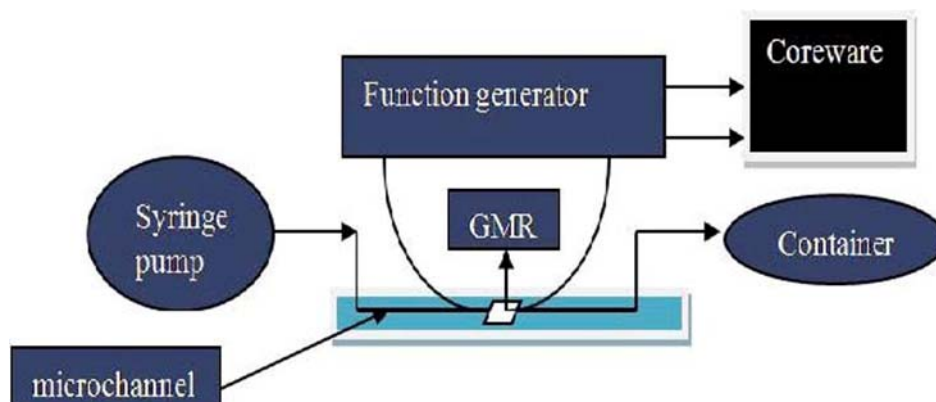


**Figure 3.2. Sensor testing schematic.**

**b. Electrodeposition of bismuth telluride (Davis)**

Nanostructured bismuth-telluride ( $\text{Bi}_2\text{Te}_3$ ) materials are the focus of intensive research since this thermoelectric material combines a high power factor and a low thermal conductivity. Thermoelectric (TE) materials can generate electricity from heat and can act as cooling devices when a voltage drop is applied. The thermo-electric phenomena provides a way to locally control temperature. Bismuth telluride ( $\text{Bi}_x\text{Te}_y$ ) nanowires were electrodeposited from aqueous acidic solutions containing different  $\text{Bi}^{3+}/\text{HTeO}^{2+}$  (20/20 mM, 20/10 mM) concentration ratios. The polarization plots predicted that combined solutions exhibit more noble reduction potentials than individual solutions. Optimized deposition potentials were obtained from the combined electrolyte polarization plots. An anomalous codeposition behavior caused increase in Te concentration for depositions in the kinetic region of bismuth telluride; otherwise decreasing Te concentrations with increased deposition potentials was observed from composition analysis. X-ray diffraction showed a dominant (110) orientation for nanowires at low deposition potentials. N-type nanowires were obtained from both electrolytes, while p-type nanowires were only obtained from the 20/10 electrolyte for low Te (< 30%) concentrations. An intrinsic to extrinsic transition was observed for nanowires deposited from 20/10 electrolyte. The highest measured Seebeck coefficient was  $-318.7 \mu\text{V/K}$  and  $117 \mu\text{V/K}$  for n-type and p-type nanowires, respectively.

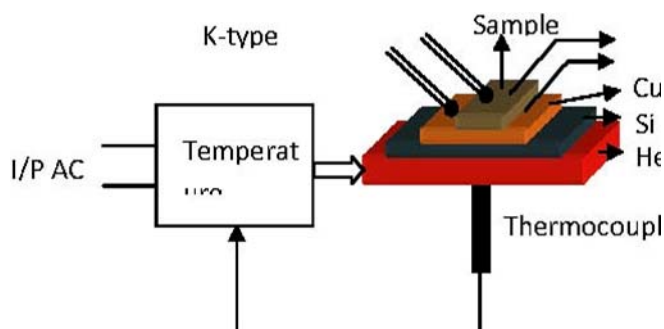


**Figure 3.3. Thermoelectric measurement device.**

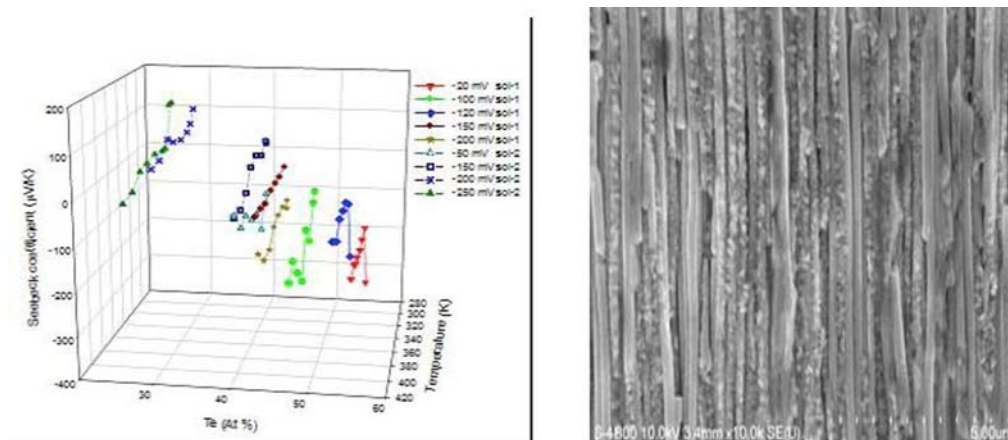


**Figure 3.4. Seebeck coefficient with respect to tellurium concentration and temperature.**

Bismuth antimony telluride ( $\text{BiSbTe}$ ) nanowires were electrodeposited at constant potentials into polycarbonate templates from a tartaric-nitric acid baths having different electrolyte compositions. Composition analysis showed that Sb deposits at higher potentials compared to  $\text{BiTe}$ . Maximum seebeck coefficients of  $337.7 \mu\text{V/K}$  and  $227.2 \mu\text{V/K}$  n-type and p-type, were obtained for nanowires samples  $\text{Bi}_{4.6}\text{Te}_{5.4}$  and  $\text{Bi}_{4.3}\text{Sb}_5$  respectively. Nonmonotonic resistance behavior was observed for all the nanowires. Figure 3.5 shows the representative SEM image of the nanowires in the background of dissolved polycarbonate template, deposited at  $-150 \text{ mV}$ . Even though the template pore diameter is  $50 \text{ nm}$ , the SEM analysis shows that the nanowires have larger average diameter of  $(110 \text{ nm} \pm 5 \text{ nm standard deviation})$ , which indicates the bulging of the nanowires in the pores during the electrodeposition process. Thermoelectric properties of

fully grown nanowires having different alloy compositions  $\text{Bi}_x\text{Te}_z$ ,  $\text{Bi}_x\text{Sb}_y$ ,  $\text{Bi}_x\text{Sb}_y\text{Te}_z$ , deposited at -250 mV from sol-A and -20 mV, -100 mV, -150 mV, -200 mV, and -250 mV from sol-B were determined.

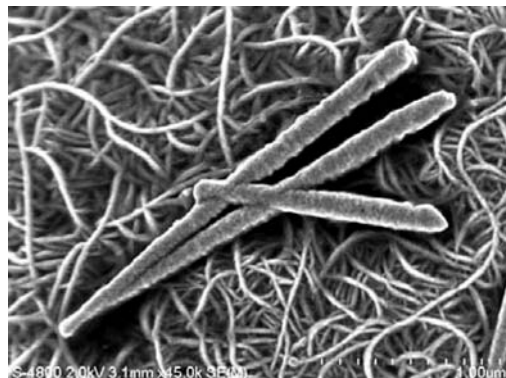


**Figure 5. SEM image of the nanowires deposited in polycarbonate membranes -150 mV.**

In conclusion, BiSbTe nanowires were successfully electrodeposited into polycarbonate template from different electrolytes. A mutually induced co-deposition mechanism was observed with the addition of Te in the electrolyte. Maximum Seebeck coefficients of  $-337.7 \mu\text{V/K}$  and  $227.2 \mu\text{V/K}$  n-type and p-type, were obtained for nanowires samples  $\text{Bi}_{4.6}\text{Te}_{5.4}$  and  $\text{Bi}_{4.3}\text{Sb}_5$  respectively. High Sb concentration negatively affected the Seebeck coefficients. More experiments are underway to study the effect of Sb and Te doping in BiSbTe nanowires.

### **c. Nanoparticle Composites (Stokes, Nolting)**

We have synthesized and measured the thermoelectric properties of several  $\text{Bi}_{2-x}\text{Sb}_x\text{Te}_3$  ( $x=0$  and  $0.5$ ) compounds as well as  $\text{Bi}_{2-x}\text{Sb}_x\text{Te}_3$ /nanoparticle composites. The nanocomposites consist of metal nanoinclusions (Bi) inside a nanostructured bulk  $\text{Bi}_{2-x}\text{Sb}_x\text{Te}_3$  matrix. Structural properties characterization has been performed by x-ray diffraction and electron microscopy. A study of the thermal and electrical properties has been completed (electrical conductivity, thermal conductivity, Seebeck coefficient and Hall effect measurements). The effect of different volume fractions of Bi nanoinclusions (3% and 5%) on the properties of the composite has been demonstrated. Figure 3.6 shows a nanocomposite which is a combination of ball-milled  $\text{Bi}_2\text{Te}_3$  with chemically-synthesized Bi nanoparticles. A transmission electron microscope cross section is shown in Fig. 3.6 (a). Thermoelectric figure of merit is shown in Fig. 3.6 (b) for three materials: the unmodified  $\text{Bi}_2\text{Te}_3$  along with  $\text{Bi}_2\text{Te}_3$ /Bi nanoparticle composites with 3% and 5% Bi nanoparticles. We found that the figure of merit of the nanocomposite ( $ZT=0.4$ ) was twice the figure of merit of  $\text{Bi}_2\text{Te}_3$  alone ( $ZT=0.2$ ). Interestingly, we found that the electrical conductivity increased due to an increase in carrier concentration but that the Seebeck coefficient did not decrease, as would be expected in a bulk semiconductor material.

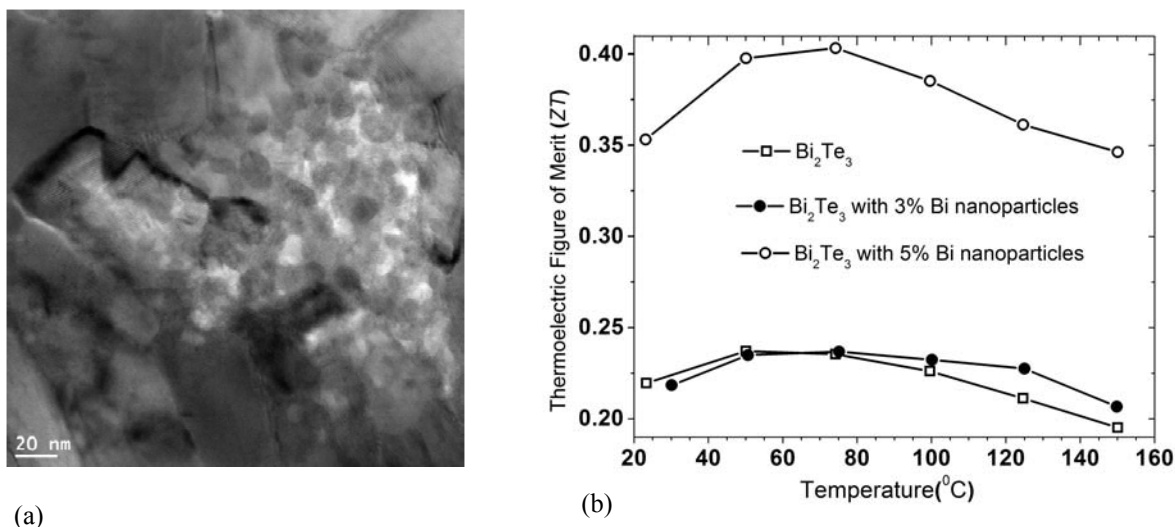


**Figure 3.6. (a) Transmission electron microscope image of Bi<sub>2</sub>Te<sub>3</sub> with Bi nanoparticle inclusions. (b) Thermoelectric figure of merit for three nanocomposites. Note the almost factor of 2 increase in the figure of merit for the nanocomposite with 5% (vol) Bi nanoparticle inclusions.**

#### **d. Thermoelectric Transport in Wires (Champagne, Karki, Walker and Young)**

This research project has focused on the synthesis and characterization of novel intermetallic systems in reduced dimensions. By measuring the magnetotransport and thermal behavior of these materials in reduced dimensions, we gain insight into the physics driving the transport properties between these low-dimensional structures and the bulk. As mentioned previously, we have been successful at coating carbon microfibers with different intermetallic systems, such as MgCNi<sub>3</sub>, Mo<sub>3</sub>Sb<sub>7</sub>, MoN, and ZnNNi<sub>3</sub>. We have recently published the work on the ZnNNi<sub>3</sub>.

Part of this project has focused on the synthesis of nanowires and nanotubes of Bi<sub>2</sub>Te<sub>3</sub> and Sb<sub>2</sub>Te<sub>3</sub> by electrodeposition (Fig. 3.7). We have previously investigated the Bi<sub>2</sub>Te<sub>3</sub> system, and just recently submitted an article for publication on the Sb<sub>2</sub>Te<sub>3</sub> wires and tubes. Scanning electron microscopy was employed to characterize the morphology and size of the fabricated Sb<sub>2</sub>Te<sub>3</sub> nanowires and nanotubes. Wavelength dispersive spectroscopy analysis confirmed the composition of the fabricated nanowires and nanotubes. The composition of the nanowires fabricated at a cathodic current density of 10 mA/cm<sup>2</sup> and nanotubes fabricated at a cathodic current density of 5.5 mA/cm<sup>2</sup> was found to be ~39% Sb and ~61% Te (2:3 ratio between Sb and Te). The fabricated Sb<sub>2</sub>Te<sub>3</sub> nanowire and nanotube arrays were found to be polycrystalline with no preferred orientation. The average lamellar thickness of the nanowires and nanotube crystallites were determined using the Scherrer equation and found to be ~36 nm and ~43 nm respectively. The Seebeck coefficient measurements at room temperature obtained for the Sb<sub>2</sub>Te<sub>3</sub> nanowires and nanotubes were +359  $\mu$ V/K and +332  $\mu$ V/K respectively, confirming that the Sb<sub>2</sub>Te<sub>3</sub> nanowires and nanotubes are *p*-type (Fig. 3.8). The high values of the Seebeck coefficients exceed that of bulk Sb<sub>2</sub>Te<sub>3</sub> crystals by almost a factor of 4, making these structures attractive for further study. Electrical resistance measurements indicated that resistance of the Sb<sub>2</sub>Te<sub>3</sub> nanowires and nanotubes decreased with increasing temperature, suggesting that these nanostructures are indeed narrow- band gap semiconductors.



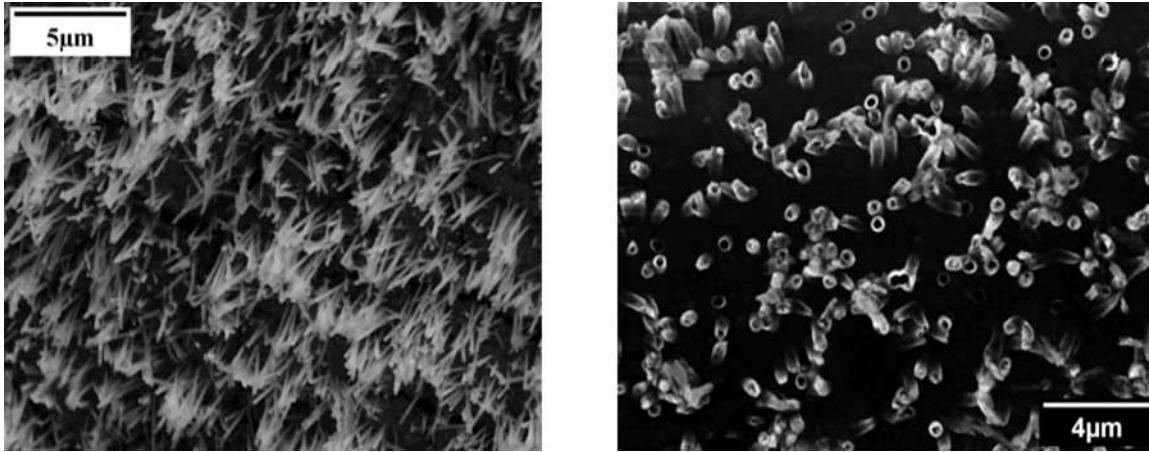


**Figure 3.7.** SEM images of arrays of electrodeposited nanowires (left) and nanotubes (right) of  $\text{Sb}_2\text{Te}_3$ .

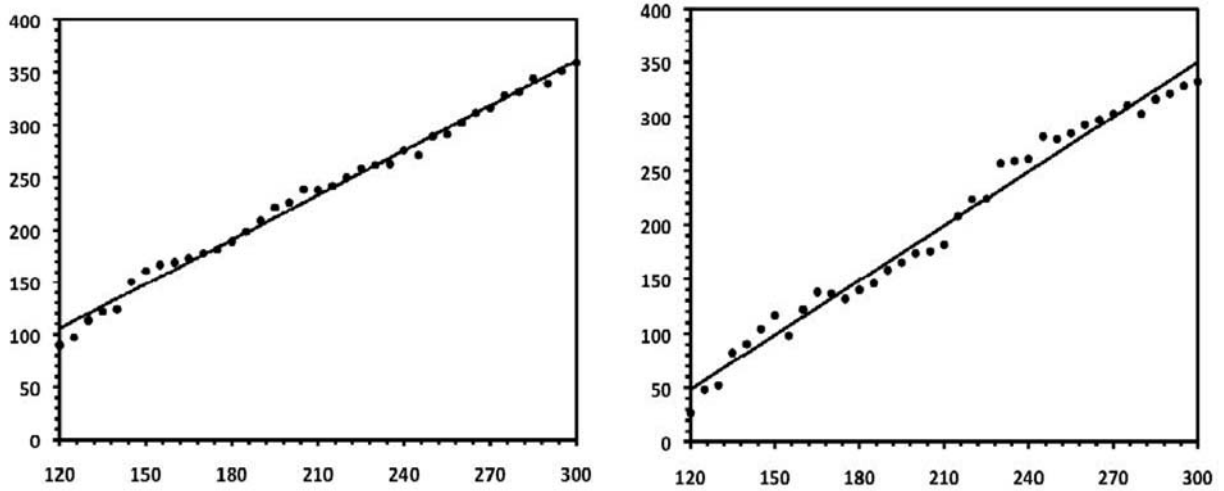


**Figure 3.8.** Temperature dependence of the Seebeck coefficients for nanowires (left) and nanotubes (right) of  $\text{Sb}_2\text{Te}_3$ .

In addition, we have begun an extensive study into the thermoelectric, transport, and magnetic properties of a series of isostructural compounds,  $TM_3$ , where  $T$  is a transition metal (Fe, Co, Ru, Rh, Os, or Ir) and  $M$  is the main group elements Ga or In. For trivalent transition metals, such as  $\text{Fe}^{3+}$  or  $\text{Os}^{3+}$ , the compounds are semiconducting. However, replacing the trivalent element with a divalent one, such as  $\text{Co}^{2+}$  or  $\text{Rh}^{2+}$  results in metallic behavior. Undoped  $\text{FeGa}_3$  has a very large and negative thermoelectric power ( $\sim -450 \mu\text{V/K}$ ), and doping with small concentrations of cobalt reduces this value, but overall produces an enhancement in the power factor ( $S^2/\rho$ ). This work on Co-doped  $\text{FeGa}_3$  will soon be submitted for publication. Our current research project in this area is focusing on  $\text{Ru}_{1-x}\text{Rh}_x\text{In}_3$ , where a metal-insulator (MI) transition exists as a function  $x$ .

This ongoing research program offers postdocs the opportunity to work on novel systems,

provides graduate students with an avenue to perform dissertation directed research, and trains undergraduates in a variety of synthesis and characterization techniques. Overall, materials synthesis provides a natural bridge between teaching and research, especially for undergraduates. They are able to make real contributions in a relatively short amount of time. Chris Champagne, an undergraduate physics major, worked last summer on the project involving  $\text{Ag}_8\text{TeGe}_6$ . He is currently a graduate student at Louisiana Tech.

#### **e. Ferroic Materials (Malkinski)**

This project deals with nonconventional methods of mutual conversion of electric to magnetic fields. One way of converting electric to magnetic field is developing multiferroic materials consisting of ferroelectric and ferromagnetic materials. More specifically, the ferroelectrics with superior electrostrictive properties can transfer over 90% of electric energy through elastic coupling to ferromagnetic materials with excellent magnetostrictive properties. The materials in the form of powders of ferroelectric PZT and PMN materials and giant magnetostrictive Terfenol powder have been purchased to make composite materials. Multiferroic composites have been fabricated consisting of a highly magnetostrictive alloy Galfenol ( $\text{Ga}_{19}\%\text{Fe}_{81}\%$ ) in the form of a powder, with grain size of 20 micrometers combined with PMN-15 relaxor type electrostrictive powder. The magneto-electronic properties of this material is being investigated. The student supported through this PKFSI grant is currently developing a new method to measure properties of bulk multiferroic composites by modifying our existing vibrating sample magnetometer. A new collaboration has been initiated between UNO (Malkinski and Stokes) and Dr. Urban, Director of NSF Institute for Polymers at the University of Southern Mississippi. The purpose of this collaborative research is to synthesize new magnetoelectric composites where the piezoelectric material will be replaced by piezoelectric polymer such as polyvinylidene difluoride -PVDF or PVDF-Tr).

#### **f. Nanoassembly of nanoparticles and tubule nanocontainers (Lvov)**

Halloysite aluminosilicate nanotubes with a 15 nm lumen, 50 nm external diameter, and length of  $800 \pm 400$  nm have been developed as an entrapment system for loading, storage, and controlled release of anticorrosion agents and biocides. Halloysite ( $\text{Al}_2\text{Si}_2\text{O}_5(\text{OH})_4 \cdot n\text{H}_2\text{O}$ ) is a two-layered tubule aluminosilicate with multilayer walls. The neighboring alumina and silica layers and their water of hydration create a packing disorder causing them to curve and roll up forming multilayer tubes. We use halloysite nanotubes with a diameter of 50 nm, lumen of 15 nm and length ca 1000 nm. The specific surface area of this halloysite is  $105 \text{ m}^2/\text{g}$ ; pore volume is  $1.30 \text{ mL/g}$ ; refractive index is 1.54; specific gravity is  $2.53 \text{ g/cm}^3$ ; and chemical composition is  $\text{Al}_2\text{O}_3$  - 36.9 %,  $\text{SiO}_2$  -48.0 %,  $\text{Fe}_2\text{O}_3$  – 0.4 %,  $\text{CaO}$  - 0.20 %,  $\text{TiO}_2$  - 0.04 %. The outermost surface of halloysite is relevant to silica, and the inner lumen surface may be compared with alumina. Halloysite tubes have  $\xi$ -potential of  $-42 \pm 2$  mV in water. Strong surface charge makes halloysite easily dispersible in polar media. Fundamental research to enable the control of release rates from hours to months is being undertaken. By variation of internal fluidic properties, the formation of nanoshells over the nanotubes and by creation of smart caps at the tube ends it is possible to develop further means of controlling the rate of release. Anticorrosive halloysite coatings are in development and a self-healing approach has been tested for repair mechanisms

through response activation to external impacts. Applications of halloysite as nanometer-scale containers are also discussed including the use of halloysite clay tubes for sustained corrosion inhibitors release, for bone implant composites, and for chemical separations. Halloysite nanotubes are available in thousands of tons, and remain sophisticated and novel nanomaterials which can be used as smart nano-containers. Halloysite is also a "green" material and due to the fact that it is a natural product will not add risk to the environment.

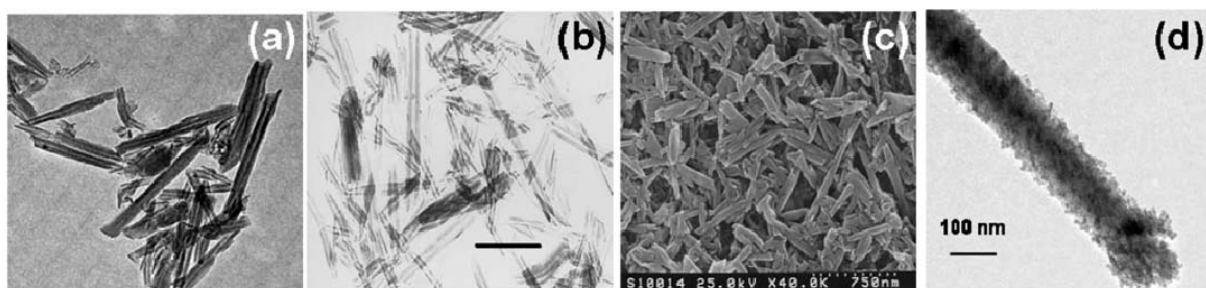


**Figure 3.9.** Transmission electron microscope images of halloysite nanotubes dispersed in water (a-b), SEM image of layer-by-layer nanocoating with halloysite multilayer (c), and halloysite nanotube coated with polyelectrolyte + 7 nm diameter silica

Halloysite nanotubes loaded with corrosion inhibitor benzotriazole can be admixed into paint to improve its anticorrosion performances as well as the coating tensile strength. Corrosion protection of such coating was evaluated by direct exposure of the coated metal (copper) substrates to highly corrosive media. Loading and release characteristics of benzotriazole from these nanotubes were studied. Benzotriazole release kinetics corresponds to the time needed for formation of metal protective layer through copper complexation. For formation of the tube end stoppers, benzotriazole loaded halloysite was exposed to the solution of Cu(II) ions, and kinetics of the stopper complex formation was analyzed. Tunable release of benzotriazole was achieved by controlling the strength of the stopper complexes, and it may be varied from ten to hundreds hours. A possibility for the tube on/off release switch was demonstrated.

New self-healing technologies for composite materials will reduce the downtime and repair costs of high performance systems as well as potentially reduce system weight by reducing overdesign. For composites used in missile systems, where the graphite composite motor cases are fabricated using a case-on-propellant manufacturing technique, any self-healing strategy must employ a non-catalytic self-healing solution, as the composite may come in contact with flammable material used in the solid rocket motor. This program will develop a self-healing composite for use in filament wound missile applications based on halloysite clay nanotubes filled with a solvent/epoxy blend for healing. We have prepared a proposal for the DoD on this topic based on our preliminary results.

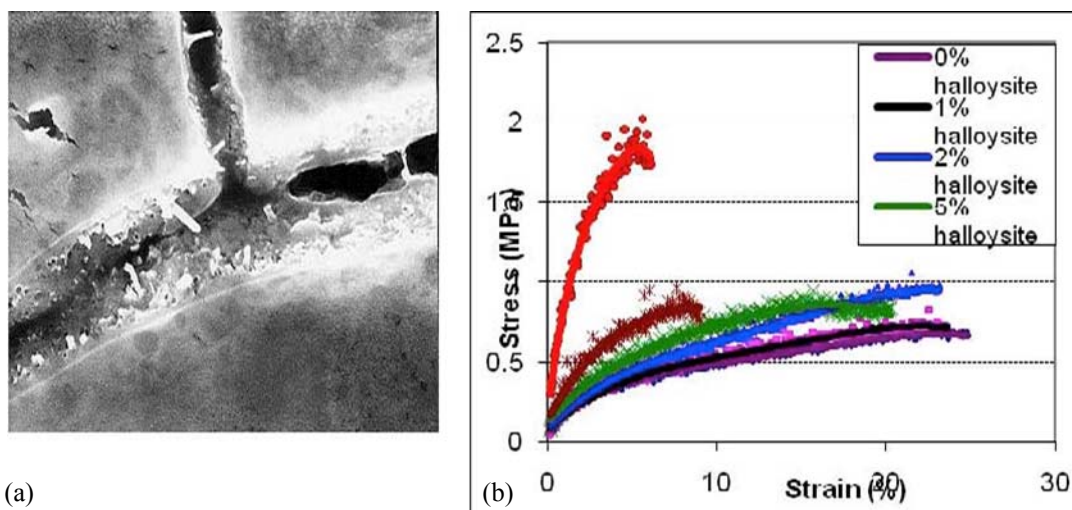


**Figure 3-10. (a) Scanning electron microscope image of cracks in dry layer of the composite with inclusion of 5 wt % halloysite nanotubes (b) Stress-strain relationship of halloysite / epoxy composite.**

#### **New project in response to Louisiana Gulf oil spill: Selective Hydrocarbon Grafting of Halloysite Lumen to Produce Inorganic Micelle-like Petroleum Sorbent Material**

The composition difference between external ( $\text{SiO}_2$ ) and internal ( $\text{Al}_2\text{O}_3$ ) halloysite wall surfaces allows selective chemical modification of the tube interior to make it hydrophobic. With this we will create inorganic nanomaterial having properties of micelle which will selectively adsorb hydrophobic impurities from water. This selective lumen treatment will be performed with phosphoric fatty acids, such as  $\text{CH}_3\text{H}_2\text{PO}_4(\text{CH}_2)_{3-17}\text{CH}_3$  or with polyphosphates. After halloysite cavity which is ca 30-40 % of the total volume is filled with oil, it may be recycled by washing out oil with gasoline or kerosene. One tone of halloysite may adsorb ca 100 kg of oil. Halloysite nanotubes are natural clay material which is mined in USA in the amount of ca 50,000 ton per year, and its' price is ca 5-10 per kg depending on purity and costs of the chemical modification. Halloysite is a "green" material and due to the fact that it is a natural product will not add risk to the sea environment. Figure 3.10 shows a TEM image of the halloysite and a schematic illustration showing the grafting of phosphoric fatty acids into lumen of halloysite and adsorption and controlled release hydrophobic impurities (e.g. petroleum pollutants). This work will be developed in the following year as response to environmental disaster. A detailed proposal on this will be developed and first experiments will begin in July-August.

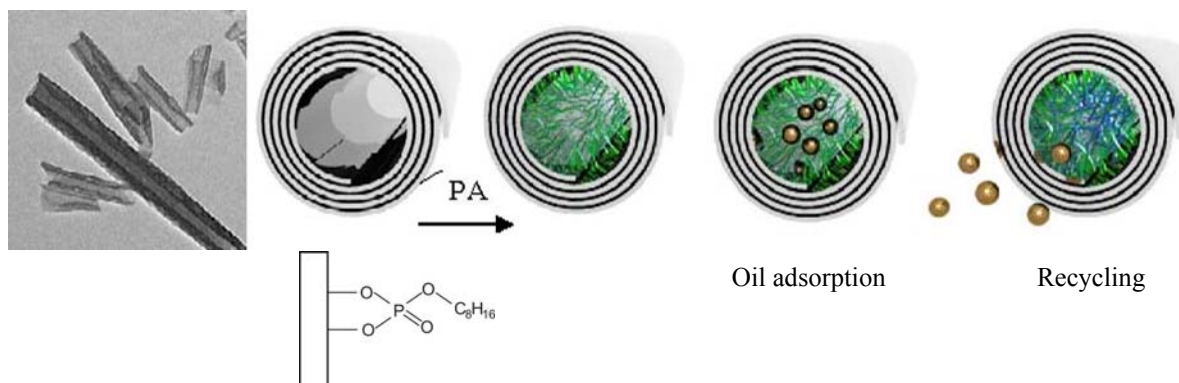


**Figure 3.11. Oil sequestering and recycling scheme based on environmentally-friendly halloysite nanotubes.**

### Partnership Activities

- Stokes (UNO) continues to work with Nanohmics, Inc. (Austin, TX) and United Technologies Research Center on a project concerning flexible thermoelectric devices.
- Dr. Lvov –AMRI annual conference in February 2010, and discussed results with AMRI researchers. Two joint reports were presented at AMRI Mardi Gras symposium. Our clay nanotube samples loaded with silver were prepared for TEM study at AMRI in collaboration with K.L. Stokes.
- A new collaboration has been initiated between UNO (Malkinski and Stokes) and Dr. Urban, Director of NSF Institute for Polymers at the University of Southern Mississippi. A joint proposal to the NSF was submitted in Feb. 2010, titled "Collaborative Research: Negative Index of Refraction Metamaterials with Chiral Nanostructures," \$265,000 (UNO).

### 3. Contributions

- Papers published: 15 papers published in scientific journals covering areas of nanoscience and nanotechnology, functional materials, materials science, physics and electrochemistry.
- Conference presentations: 30 presentations at national and international scientific conferences. Some selected notable presentations are listed below.
  - E. Abdullayev (Lvov, IfM)- Award for the Best Student Poster at 29th Biennial Western Coating Symposium, Las Vegas, NM, October 28, 2009.
  - Debasish Mohanty (Gabrish, UNO) - First Place Poster Competition at the 215th Electrochemical Society meeting in San Francisco, CA, May 24-May 29, 2009.
  - S. Sumithra (Stokes, UNO) Poster – Nominated for Best Poster award, 2009 Materials Research Society Fall Meeting, November 30-December 4, 2009, Boston, MA.
- Grants and Contracts/Economic Development: Several grants and contracts which have used data and/or ideas generated from the PKSFI research have been received including:
  - Biofuel: Nanoreactors for ethanol production, Y. Lvov, co-PI, Department of Energy, \$300,000; Nov 1, 2008 – July 31, 2010

- SBIR Phase II: Compact night vision focal plane array cooling using FlexTEC high-ZTape, K. Stokes, co-PI, Army Research Office/Nanohmics, Inc., Austin TX. \$750,000 Jan 2009 to Mar 2011.
  - Women in Engineering, D. Davis, co-PI. NSF \$750,000, Sept 2009-Aug 2012
  - Pending Proposals: 9 Individual and/or multi-PI Federal proposals which use data generated from this PKSFI-FRG. Agencies include NSF (including NSF-EPSCoR RII), NASA, Dept. of Energy and NIH.
- Student Outcomes: Six graduate students and two undergraduates directly supported (Physics, Chemistry, Nanosystems Engineering). There were two PhD graduates (Engineering, LATech). In addition, four summer students supported on other grants (REU) worked on PKSFI-related projects.
  - Constructed a high-temperature probe for measuring the Seebeck coefficient. The probe is used in conjunction with a Lindberg/Blue M small tube furnace. Data are collected with nanovoltmeters, and the program is controlled by LabView software.

#### 4. Project Revision

Dr. Heike Gabrisch left the University of New Orleans in March 2010. After consultation with the lead-PI (O'Connor) and other Focused Research Group leaders, it was decided that Dr. Ferdinand Poudeu will now be part of FRG #3. His research will be in the area of thermoelectric nanocomposites and compliments the on-going research of Stokes, Davis and Young.

#### 5. Work Products

##### Papers:

- [1] E. Abdullayev, R. Price, and Y. Lvov, "Halloysite Tubes as Smart Nanocontainers for Anticorrosion Agent Benzotriazole," *ACS Applied Materials and Interfaces*, vol. 2, pp. 1437-1442, 2009.
- [2] R. Bellamkonda, T. John, B. Mathew, M. DeCoster, H. Hegab, J. Palmer, and D. Davis, "Microfabrication of nanowires-based GMR biosensor," in *Proceedings of SPIE, Micro- and Nanotechnology Sensors, Systems, and Applications* vol. 7318 Bellingham, WA: SPIE, 2009, p. 73181H.
- [3] R. Bellamkonda, T. John, B. Mathew, M. A. DeCoster, H. Hegab, and D. Davis, "Fabrication and testing of a CoNiCu/ Cu CPP-GMR nanowire-based microfluidic biosensor," *Journal of Micromechanical Microengineering*, vol. 20, p. 025012, 2010.
- [4] D. Fix, Y. Lvov, and D. Shchukin, "Application of Inhibitor Loaded Halloysite Nanotubes in Active Anticorrosive Coatings," *Advanced Functional Materials*, vol. 19, pp. 1720-1727, 2009.
- [5] P. Garrity and K. L. Stokes, "Thermal Noise as a Spectroscopic Tool to Determine Transport Properties," *Philosophical Magazine*, vol. 89, pp. 2129-2147, 2009.
- [6] P. L. Garrity and K. L. Stokes, "Direct Measurement of the Absolute Seebeck Coefficient for Pb and Cu at 300 K to 450 K," in *Thermoelectric Materials—Growth, Properties, Novel Characterization Methods, and Applications, Mater. Res. Soc. Symp. Proc.* vol. 1267, J. D. Baniecki, Ed. Warrendale, PA: MRS, 2010, pp. 1267-DD11-0.
- [7] N. Haldolaarachchige, W. A. Phelan, J. Y. Chan, and D. P. Young, "Chemical Doping

- Effect on Thermoelectric Properties of Intermetallic Narrow Band Semiconductors (TMGa<sub>3</sub>: TM = Fe, Ru & Os)," *Journal of Applied Physics*, **to be submitted**, 2010.
- [8] A. B. Karki, Y. M. Xiong, D. P. Young, and P. W. Adams, "Superconducting and magnetotransport properties of ZnNi<sub>3</sub> microfibers and films," *Physical Review B*, vol. 79, p. 212508, 2009.
  - [9] D. Pinisetty, M. Gupta, A. B. Karki, D. P. Young, and R. V. Devireddy, "Fabrication and Characterization of Electrodeposited Antimony Telluride Nanowires and Nanotubes," *Chemistry of Materials*, **submitted**, 2010.
  - [10] S. Sumithra, D. K. Misra, C. Wei, H. Gabrisch, P. F. P. Poudeu, and K. L. Stokes, "Solvochemical synthesis and particle size distribution analysis of Bi, Sb and Bi<sub>0.88</sub>Sb<sub>0.12</sub> nanoparticles," *Journal of Nanoparticle Research*, **submitted**, 2010.
  - [11] S. Sumithra, N. J. Takas, N. L. Henderson, W. M. Nolting, D. M. Misra, P. F. P. Poudeu, and K. L. Stokes, "Metal Nanoinclusions (Bi and Ag) in Bi<sub>2</sub>Te<sub>3</sub> for Enhanced Thermoelectric Applications," in *Thermoelectric Materials—Growth, Properties, Novel Characterization Methods, and Applications*, Mater. Res. Soc. Symp. Proc. vol. 1267, J. D. Baniecki, Ed. Warrendale, PA: MRS, 2010, pp. 1267-DD07-11.
  - [12] S. Sumithra, N. J. Takas, D. M. Misra, P. F. P. Poudeu, and K. L. Stokes, "Nanocomposites of Bi<sub>2</sub>Te<sub>3</sub> with Metal Nanoinclusions for Advanced Thermoelectric Applications," in *Energy Harvesting - From Fundamentals to Devices*, Mater. Res. Soc. Proc. vol. 1218E, H. Radouski, J. D. Holbery, L. H. Lewis, and F. Schmidt, Eds. Warrendale, PA: MRS, 2009.
  - [13] V. Vergaro, E. Abdullayev, R. Cingolani, Y. Lvov, and S. Leporatti, "Cito/biocompatibility and Uptake for Clay Nanotubes," *Biomacromolecules*, vol. 11, pp. 820-828, 2010.
  - [14] C. Yelleswarapu, E. Abdullayev, Y. Lvov, and D. Rao, "Nonlinear Optics of Nontoxic Nanotubes," *Optics Communications*, vol. 283, pp. 428-441, 2010.

#### **Presentations:**

- [1] Y. Lvov, R. Price, and E. Abdullayev, "Halloysite- benzotriazole nanocomposites, low cost additives to metallic coatings for corrosion protection," in *29<sup>th</sup> Biennial Western Coating Symposium*, Las Vegas, NV, October 25-28, 2009
- [2] S. Sumithra, N. J. Takas, N. L. Henderson, W. M. Nolting, D. K. Misra, P. F. P. Poudeu, and K. L. Stokes, "Effect of Metal Nanoinclusions in bulk Bi<sub>2-x</sub>Te<sub>3+x</sub> and Bi<sub>0.5</sub>Sb<sub>1.5</sub>Te<sub>3</sub> system," in *Materials Research Society Symposium*, San Francisco, CA, April 4-9, 2010.
- [3] K. L. Stokes, "Progress in PKSFI Focused Research Group 3: Energy Conversion and Storage Materials," in *12<sup>th</sup> Annual DARPA-AMRI Symposium and Review*, New Orleans, LA, Feb. 11-12, 2010.

#### **Report of Inventions:**

- [1] D. Mills and Y. Lvov, "Smart Bioactive Nanocoating with Sustained Drug Release Capability for Implants, Wound Repair and Tissue Regeneration," April 23, 2010. ROI #2010-08
- [2] Y. Lvov, "Selective Hydrocarbon Grafting of Halloysite Lumen to Produce Inorganic Micelle-like Petroleum Sorbent Material," May 14, 2010. ROI #2010-12



## PKSFI Report for LEQSF(2007-12)-ENH-PKSFI-PRS-04

**Matthew A. Tarr**  
**(PKSFI Broader Impacts, 2009-2010)**

### **Broader Impacts (Educational and Commercial Outreach)**

1. **Personnel:** List all key personnel and other staff who provided *significant* contributions to the project. Provide information about the types of contributions made by each listed participant and controls in place to ensure that these contributions are adequate to the project's requirements.

Matthew Tarr, Professor, Dept. of Chemistry, University of New Orleans – planned and coordinated academic year outreach activities (ScienceREACH program) with subcontractor, Communities In Schools of New Orleans (CISNO); reviewed CISNO quarterly reports; presented program updates at quarterly meetings; conducted site visit to CISNO to evaluate subcontractor progress; coordinated planning and recruiting for summer outreach program; supervised by project PI, Dr. Charles O'Connor.

Sara Massey, Director, Communities In Schools of New Orleans – directed all activities carried out by CISNO including academic year outreach programs in New Orleans public or charter schools; responsible for hiring and supervising ScienceREACH program coordinator; evaluated via quarterly reports submitted to Dr. Tarr and by site visits conducted by Dr. Tarr.

Deidra Schauer, ScienceREACH Coordinator, Communities In Schools of New Orleans – implemented academic year outreach activities; directly supervised and evaluated by Sara Massey.

### **2. Activities and Findings:**

- Describe major research and educational activities undertaken in this reporting period

This portion of the project included two components: 1) a summer research program for high school students and 2) an academic year support program (ScienceREACH) for high school students.

The summer research program hosted 12 high school student participants during the summer of 2009 and 10 high school student participants during the summer of 2010. Each participant conducted research on an independent project in chemistry, physics, materials science, biology, or psychology. In addition, weekly seminar programs allow for discussion of current scientific issues, general research concepts, and scientific ethics.

During this project year, the ScienceREACH program worked in five schools; McMain Secondary School, Sarah T. Reed High School, George W. Carver High School, Walter L. Cohen High School and John McDonough High School. The programs implemented included: Rocketry Program, Forensics Program, in-class presentations, field trips, in-class assistance, college assistance and tutoring as well as mentoring, which combined reached a total of 263 students across 82 sessions vs. 204 students last year, representing a 30% increase.

- Describe and provide data supporting the major findings resulting from these activities

The summer research component of this project hosted 12 high school student participants in the summer of 2009. A summary of representative student research projects is given below.

**Kewe Ukpolo, Synthesis of TiO<sub>2</sub> nanowires by hydrothermal method**

Titania (TiO<sub>2</sub>) is getting more attention in recent years as it can exhibit a wealth of important photovoltaic, semiconductor photo-catalyst, catalytic support and gas-sensing properties especially when prepared as nanomaterials. Nanowires are essentially shrunken down versions of modern day wires and are made of various metals. We believe by creating nanowires out of titania we can UV protection more efficient, can also reduce the cost of making solar cells, and also make Photocatalysis (photocatalytic activity of titania results in the material exhibiting self cleaning and disinfecting properties under exposure to UV radiation.) In this research we investigate the effect of the parameters (reagent, duration, concentration etc.) on the morphologies of TiO<sub>2</sub> nanowires. We also achieved thin TiO<sub>2</sub> nanowires by hydrothermal process. The synthesis and characterization of these novel analogs will be presented.

**Corinne Bachaud, Differences in Magnetic Signatures of Various Types of Music on Cassette Tape**

This experiment was conducted to observe differences in the magnetic signature of different types of music recorded on the magnetic tape in an audio cassette. The types of music tested include heavy metal, techno, acoustic, classical, and hip-hop, as well as a control with no music at all. The samples were tested on the Vibrating Sample Magnetometer to find any differences in the starting points of the magnetic graphs. These starting points varied quite a bit from each sample. The sample was then measured with the Magnetic Force Microscope to observe any differences in the magnetic domain images, of which there were very few, most likely due to a magnetic component of the machine.

**Arianna E. Rivera, Synthesis and Characterization of the Quaternary Selenides FeSn<sub>3</sub>Bi<sub>4</sub>Se<sub>10</sub> and NiPb<sub>3</sub>M<sub>4</sub>Se<sub>10</sub> (M = Sb, Bi)**

Three new quaternary mixed metal selenides with compositions FeSn<sub>3</sub>Bi<sub>4</sub>Se<sub>10</sub>, NiPb<sub>3</sub>Bi<sub>4</sub>Se<sub>10</sub> and NiPb<sub>3</sub>Sb<sub>4</sub>Se<sub>10</sub> were synthesized via solid-state reactions involving elemental Fe, Ni, Sn, Pb, Sb, and Se at 500°C. Powder X-ray diffraction (PXRD) and Differential Scanning Calorimetry (DSC) suggested that all the reaction products were single phase. The compounds melt incongruently with onset temperatures at 629 °C, 685 °C and 574 °C for FeSn<sub>3</sub>Bi<sub>4</sub>Se<sub>10</sub>, NiPb<sub>3</sub>Bi<sub>4</sub>Se<sub>10</sub> and NiPb<sub>3</sub>Sb<sub>4</sub>Se<sub>10</sub> respectively. Electronic charge transports measurements on FeSn<sub>3</sub>Bi<sub>4</sub>Se<sub>10</sub> and NiPb<sub>3</sub>Bi<sub>4</sub>Se<sub>10</sub> indicated that both phases are n-type semiconductors with room temperature electrical conductivity and thermopower values of 0.254 S/cm and -62.5 μV/K for FeSn<sub>3</sub>Bi<sub>4</sub>Se<sub>10</sub>; and 709 S/cm and -52 μV/K for NiPb<sub>3</sub>Bi<sub>4</sub>Se<sub>10</sub>.

The ScienceREACH component of this project reached a total of 204 students across 225 different sessions.

**(1) Rocketry After School Program:** This program continued from last year, and was conducted at McMain Secondary School. In the Spring of 2010, David Koscielniak, a mentor from the National Association of Rocketry, is assisting students in designing and building their competition rockets. Students also designed and built bottle rockets and model rockets and launched them. The program served a total of 40 students, and was held for 10 mentoring sessions this quarter and will continue in the spring.

**(2) Forensics After School Program:** The Forensics Program has also continued from last year. The program met seven times between August 2009 and November 2009; there were 35 students involved in 5 sessions. The students worked in different areas of Forensics, such as: DNA Analysis, Forensics labs, which included pH Testing and Fingerprint analysis, Forensic Math, Forensic Anthropology, Handwriting Analysis, Computer Forensics, and Blood Typing. Detective Tanisha Santemore, a Forensic Scientist/Criminologist II, taught students how to investigate a crime scene, collect evidence, and analyze evidence in a lab. In addition, the students participated in various experiments about data collection.

**(3) In-Class Presentations:** Between September 2009 and November 2009 there were 3 In-Class Presentations. 1 Loyola Service Learner, 5 Xavier Service Learners, and 3 Tulane Service Learners gave students a presentation about college life. The college students and the high school students met in small groups so that the high school students could ask questions about scholarships, the admissions process, and college life. They presented to 80 students during 7 sessions in Mr. Brown's Physical Science class, Mr. Peace's Biology class, and Mr. Crooks Math GEE class. The presenters talked to the students about college, careers in health sciences, and spoke specifically about their chosen majors.

**(4) Field Trips:** In addition to exposing students to a variety of STEM fields, ScienceREACH has expanded the field trip component in order to increase students' hands on experiences in areas of interest to them. As part of this there were four field trips between September 2009 and November 2009. Students from Sarah T. Reed and Walter L. Cohen visited the science departments at Xavier University of Louisiana. Dr. Anderson Sunda-Meya, a physics professor at Xavier did four presentations to 195 students on Nanotechnology. Visiting students also participated in 8 demonstrations conducted by the Xavier's physics majors. Students ended the visit with a campus tour and eat lunch and ask questions about majors in the STEM fields.

**(5) Tutoring/ Mentoring:** Gabriel Fette, the ScienceREACH AmeriCorps member, Catherine Cresson, and service learners from Delgado Community College, Tulane University, Loyola University, and Xavier University have tutored at George W. Carver High School, Eleanor McMain High School, John McDonough High School, and Sarah T. Reed High School this quarter. The services were as follows:

- Reed - 28 students for a total of 24 hours on 12 days
- Cohen - 60 students for a total of 129 hours on 31 days,
- McMain - 6 students for a total of 30 hours on 15 days
- John Mac - 32 students for a total of 12 hours on 6 days.
- Carver- 26 students for a total of 36 hours on 18 days

In addition to individual tutoring and mentoring, Gabriel Fette, Catherine Cresson, and the service learners have provided in-class assistance by being additional support for the students as well as helping teachers with labs and experiments. In addition to using the service learners at Delgado, Loyola, Tulane, and Xavier, ScienceREACH is planning to incorporate service learners from Dillard University and the UNO STARS from University of New Orleans into the tutoring and mentoring curriculum.

**(6) College Assistance:** The ScienceREACH Coordinator worked individually with students helping them pick colleges that had a science curriculum best suited to their needs, and helped them map out their college classes and requirements. This fall ScienceREACH introduced the scholarship component of the college assistance curriculum. Sara Massey and Deidra Schauer attended the National Scholarship Providers Association Convention in New Orleans, LA. ScienceREACH is now equipped to customize scholarships to fit the students' needs as well as utilize a database that will expose students to scholarships on a local, regional, and national level. The scholarship information and assistance has been shared with juniors and seniors at Sarah T. Reed High School, Eleanor McMain High School, and Walter L. Cohen High School.

ScienceREACH is adding one new component to the curriculum. The Science of Sport, which was developed by Gabriel Fette, will encourage outdoor activity while reinforcing grade level expectations. This program will expose the students to careers in the health sciences. In this program we aim to serve more than 150 students at Carver High, Cohen High and John McDonogh High.

- Describe the opportunities for faculty recruitment, retention and development, as well as post-doc, graduate and undergraduate student training provided by your project

There have been multiple interactions with UNO Personnel. The ScienceREACH Coordinator continues to cultivate the relationship with the UNO STARS Program. The Coordinator continues to work with the UNO Admissions Office in order to plan for a UNO Admissions counselor to be present at the college day.

ScienceREACH also continues to work with UNO's Upward Bound Program to provide the STEM enrichment portion of the Upward Bound Summer Program.

- Describe the nature and scope of partnership activities

CISNO served as the primary agency for design, coordination, and implementation of all academic year outreach activities as described above.

- Describe any problems encountered during the last year of project activities.

No problems were encountered.

**3. Contributions:** Summarize efforts made to build research and education capacity, secure external federal and private-sector funding, build infrastructure, contribute to economic development, and ensure project sustainability over the long term.

Summer research programs substantially impact the education and career paths of high school participants. Many of our participants go on to study science or engineering in college. This influx of students helps to provide future employees in STEM fields.

Academic year outreach programs were designed to attract high school students into college study in science and engineering fields. All schools targeted in this study have student bodies that are majority African-American. Furthermore, these schools have a high percentage of students receiving reduced or free lunch. Developing these human resources will provide a stronger base for science and technology development within the state of Louisiana.

**4. Project Revision:** Provide a listing of and explanation for any significant changes in the work plan for upcoming year, including any changes in the amount of investigators' time devoted to the project. If you made significant changes to the project design as outline in the proposal during the past year, please list and explain the changes, the purposes for the changes, and the results.

Several programs developed by CISNO will continue to be implemented in project year four. Refining of these programs will be undertaken in order to make them more efficient, but no major changes are foreseen. Efforts will be made to increase the number of undergraduate students involved in the project.

**5. Work Products:** List any tangible products (e.g., research publications and/or presentations, patents, licensing agreements etc.). Please combine all products into one document.

**"Synthesis and Characterization of the Quaternary Selenides of  $\text{FeSn}_3\text{Bi}_4\text{Se}_{10}$  and  $\text{NiPb}_3\text{M}_4\text{Se}_{10}$  ( $\text{M}=\text{Sb}, \text{Bi}$ ),"** Arianna E. Rivera, Ronald J. Coats Jr., Nathan J. Takas, Clarence J. Anglin, P. Ferdinand P. Poudeu, Student Research Poster Session, American Chemical Society Louisiana Local Section, September 30, 2009, University Center Ballroom, Xavier University of Louisiana, New Orleans, LA.

**PKSFI Report for LEQSF(2007-12)-ENH-PKSFI-PRS-04**  
**Leszek M. Malkinski**  
**(PKSFI-ESIP Clean Room, 2009-2010)**

**Title: Nanodevice Processing Laboratory**

**1. Personnel:**

**Leszek Malkinski**, Associate Professor of Physics and Materials Science. Dr. Malkinski is in charge of design and management of this part of the project.

**2. Activities:**

The aim of this project is to provide research support for AMRI and collaborating institutions with the cleanroom facilities and technology to do competitive research in the field of nanofabrication. The evaluation of the purity of the air is based on number of dust particles in a unit volume. "Class 1000" cleanroom is the minimum requirement for the research activities on nanotechnology. This requirement was exceeded by designing a higher class purity cleanroom with re-circulating air. Due to this design the number of particles present in the unit volume dropped to below 100, which elevates the rank of the cleanroom to "class 100".

The Installation of the laboratory was completed in December 2008 and after testing by the independent professional contractor (ENV Services) a certificate of Compliance was issued, stating that our Nanodevice Processing Laboratory meets the ISO standards of "class 100" cleanroom.

In January, February and March 2009 the technological and measurement equipment installed and the laboratory:

- mask aligner and UV exposure station for photolithography,
- spin coater and hot plate for photoresist coating,
- ion milling system for dry etching of the patterns for devices,
- wire bonder for making electric connections with micron thick wire.
- atomic force microscope for characterizing the structure of the devices.

Also, in the same time period the laboratory was fully furnished with chairs, desks, tables and cabinets which meet class 100 cleanroom specifications.

The equipment was tested within next 3 months and in the summer 2009 first group of users of the Nanodevice Processing Laboratory has been trained in using the instruments and equipment and obeying the cleanroom rules. The remaining funds in the Nanodevice Processing Laboratory were used for the purchase of coveralls, boots and hoods for the users of the laboratory.

Currently about 20 users from AMRI received cleanroom training and are qualified for unrestricted use of the Laboratory. In addition two users from the Tulane University, from the collaborating group of Prof. Z. Mao got access to our laboratory.

The laboratory has been extensively and successfully used for realization of the PKFSI and other research projects by the faculty, postdoctoral researchers and student from UNO and collaborating institutions.